**Biogeosciences Discussions**

# Size distribution of particles and zooplankton across the shelf-basin system in Southeast Beaufort Sea: combined results from an Underwater Vision Profiler and vertical net tows

A. Forest[1], L. Stemmann[2], M. Picheral[2], L. Burdorf[2], D. Robert[1], L. Fortier[1], and M. Babin[1]

[1]Takuvik Joint International Laboratory, Université Laval (Canada) – CNRS (France), Département de Biologie and Québec-Océan, Université Laval, G1V 0A6, Canada
[2]Laboratoire d'Océanographie de Villefranche, Université Pierre et Marie Curie-Paris 6 and CNRS, 06230 Villefranche-sur-Mer, France

Correspondence to: A. Forest (alexandre.forest@takuvik.ulaval.ca)

Title Page

| Abstract | Introduction |
| Conclusions | References |
| Tables | Figures |

## Abstract

The size distribution and mean spatial trends of large particles (>100 µm, in equivalent spherical diameter, ESD) and mesozooplankton were investigated across the Mackenzie Shelf (Southeast Beaufort Sea, Arctic Ocean) in July–August 2009. Our main objective was to combine results from an Underwater Vision Profiler 5 (UVP5) and traditional net tows (200 µm mesh size) to characterize the structural diversity and functioning of the Arctic shelf-basin ecosystem and to assess the large-scale correspondence between the two methodological approaches. The core dataset comprised 154 UVP5 profiles and 29 net tows conducted in the shelf (<100 m isobath), slope (100–1000 m) and basin (>1000 m) regions of the study area. The mean abundance of total particles and zooplankton in the upper water column (<75 m depth) declined exponentially with increasing distance from shore. Vertical and latitudinal patterns in total particle concentration followed those of chlorophyll-$a$ (chl-$a$) concentration, with maximum values between 30 and 70 m depth. Based on the size-spectra derived from the UVP5 dataset, living organisms (0.1–10 mm ESD) accounted for an increasingly large proportion of total particle abundance (from 0.1 % to > 50 %) when progressing offshore and as the ESD of particles was increasing. Both the UVP5 and net tows determined that copepods dominated the zooplankton community (∼ 78–94 % by numbers) and that appendicularians were generally the second most abundant group (∼ 1–11 %). The vertical distribution patterns of copepods and appendicularians indicated a close association between primary production and the main grazers. Manual taxonomic counts and ZooScan image analyses shed further light on the size-structure and composition of the copepod community – which was dominated at ∼ 95 % by a guild of 10 typical taxa. The size distributions of copepods, as evaluated with the 3 methods (manual counts, ZooScan and UVP5), showed consistent patterns co-varying in the same order of magnitude over the upper size range (> 1 mm ESD). Copepods < 1 mm were not well quantified by the UVP5, which estimated that only ∼ 13–25 % of the assemblage was composed of copepods <1 mm ESD compared with ∼ 77–89 % from

Full Screen / Esc

Printer-friendly Version

Interactive Discussion

the net tow estimates. However, the biovolume of copepods was overwhelmingly dominated (∼ 93–97 %) by copepods >1 mm ESD. Our results illustrate that the combination of traditional sampling methods and automated imaging techniques is a powerful approach that enabled us to conclude on the prevalence of a relatively high productivity regime and dominant herbivorous food web over the shelf when compared with the low-productive recycling system detected offshore.

# 1 Introduction

Particles in aquatic systems can be divided in two fundamental groups: living and non-living. Size of non-living particles (named marine snow for sizes > 500 µm; Suzuki and Kato, 1953) is the net result of aggregation and destruction processes, which include a large variety of physical and biological mechanisms such as coagulation, packaging, consumption, dissolution and fragmentation (see Burd and Jackson, 2009 for a review). The particle size distribution (PSD) of non-living particles is particularly instructive for vertical flux studies if the settling velocity of observed particles is known (e.g., McDonnell and Buesseler, 2010) or if the PSD can be related to sediment trap measurements (e.g., Guidi et al., 2008; Iversen et al., 2010). In turn, numerical models of biogeochemical fluxes used simplified PSD to estimate the magnitude and timing of sinking particle flux events (e.g., Kriest and Evans, 2000; Stemmann et al., 2004; Karakas et al., 2009). However, the strength and efficiency of the biological pump are closely connected to the aforementioned transformation processes in the water column, which are indeed largely driven by planktonic communities, including bacteria, protists and metazoans (e.g., Wassmann et al., 2003; Forest et al., 2011; Jackson and Checkley, 2011; Kellogg et al., 2011). Therefore, knowledge on the contribution of living particles to the total particle pool and on the plankton size distribution is essential if the dynamics of downward carbon export *and* trophic energy fluxes are to be adequately understood and modeled in marine ecosystems. Information on the variability of the size spectrum of particles supports the characterization of various ecological processes and is key to

our comprehension of the structure and function of pelagic food webs (e.g., Platt and Denman, 1978; Legendre and Michaud, 1998; Stemmann and Boss, 2012).

The PSD of living particles (i.e. plankton) is recognized to be useful for describing the structural properties of a given marine food web. When converted into biomass, variations in the slope of the normalized PSD on a logarithmic scale can be linked to efficiencies in both the energy transfer to higher trophic levels and vertical carbon export to depth (e.g., Guidi et al. 2009; Frangoulis et al., 2010). Anomalies in the shape of the log-transformed plankton size distribution may also be indicative of excess growth/mortality or gain/losses through consumption or migration (Zhou et al., 2006; Frangoulis et al., 2010). Furthermore, size-based analysis of living particles provides a valuable tool in ecosystem modeling for reducing the complexity of actual food webs and species interactions (Zhou et al., 2010). For example, size-structured ecosystem models can unravel shifts in the diet of zooplankton when the latter grow, since large organisms usually consume smaller ones (Platt and Denman, 1978). Species-oriented or functional group modeling approaches of trophic networks cannot solve this issue (Moloney et al., 2010). This is particularly true for Arctic regions where marine ecosystems experience marked seasonal variability in biological productivity as a direct consequence of physical conditions (e.g. light, temperature). As a result, Arctic zooplankton can rapidly change their food regime depending on the nature and availability of organic matter in their environment. In fact, even the large calanoid species *Calanus hyperboreus* and *C. glacialis* that typically dominate the biomass in the Arctic Ocean – and which are traditionally known to be herbivore (Darnis et al., 2008; Falk-Petersen et al., 2009) – appear to have a much more flexible diet (e.g. fecal pellets, detritus, microzooplankton) than initially believed (e.g., Seuthe et al., 2007; Campbell et al., 2009; Sampei et al., 2009).

This study investigated the PSD of large particles $> 100\,\mu\text{m}$ (total and zooplankton, expressed in equivalent spherical diameter, ESD) across the shelf-slope-basin interface in the Southeast Beaufort Sea (Arctic Ocean) in late July/August 2009 (Fig. 1). Our main goal was to combine results from an Underwater Vision Profiler 5 (UVP5,

**Particles and zooplankton in Beaufort Sea**

A. Forest et al.

Title Page

Abstract | Introduction

Conclusions | References

Tables | Figures

|◄ | ►|

◄ | ►

Back | Close

Full Screen / Esc

Printer-friendly Version

Interactive Discussion

Picheral et al., 2010) and from traditional net tows to infer the structure and functioning of an Arctic shelf ecosystem during the late summer season. Our specific objectives were (1) to document with high-vertical resolution imaging techniques the large-scale trends of PSD and particle concentration across the shelf-basin boundary; (2) to examine the degree of similarity between the zooplankton dataset acquired with the UVP5 and the one obtained using standard vertical net tows; (3) to characterize the size spectra of total particles and zooplankton in an ecosystem known for its relatively low diversity; and (4) to set the stage for a comprehensive study on vertical particle fluxes and ecosystem dynamics in the Southeast Beaufort Sea during post-bloom conditions.

## 2  Material and methods

### 2.1  Study area and sampling strategy

The Mackenzie Shelf (Fig. 1) is a relatively narrow Arctic shelf (width $\sim 120$ km, length $\sim 530$ km) covered with ice from October until May to early August, reaching a maximum thickness of 2–3 m in March/April (Barber and Hanesiak, 2004). The Mackenzie River supplies $\sim 330$ km$^3$ yr$^{-1}$ of freshwater and $124 \times 10^6$ t yr$^{-1}$ of sediment on the shelf (Gordeev, 2006). Approximately 75 % of the total annual discharge is delivered between May and September, with a typical peak in June. As the summer progresses, both river runoff and ice melt contribute to build up a strongly stratified surface layer in the top 5–10 m (Carmack and Macdonald, 2002). Saltwater masses in the region comprise the Polar-Mixed Layer (salinity < 31, $\sim 0$–50 m depth), the Pacific Halocline ($\sim 31$–33, $\sim 50$–200 m), and deep waters of Atlantic origin ($\sim 34.5$, > 220 m) (Lansard et al., 2011). Surface circulation is variable and linked to ice and wind conditions (Ingram et al., 2008). Inshore, a typical coastal current flows from west to east, whereas offshore surface circulation is overall influenced by the anti-cyclonic Beaufort Gyre (Ingram et al., 2008).

Full Screen / Esc

Printer-friendly Version

Interactive Discussion

Primary production in the Beaufort Sea usually ranges from 30 to 70 g C m$^{-2}$ yr$^{-1}$, indicative of oligotrophic conditions (Sakshaug, 2004; Carmack et al., 2004). The spring bloom rapidly evolves into a subsurface chlorophyll maximum (SCM) as a result of relatively low nitrate concentrations in the surface layer at the end of winter (Tremblay et al.,
5   2008). Over the growth season, the SCM progressively lowers the nitracline down to ∼ 60 m depth where light becomes the limiting factor (Martin et al., 2010). A second phytoplankton bloom can occur in late summer or in the fall as a result of wind-driven mixing and/or coastal upwelling (Brugel et al., 2009).

    Data used in the present study were collected across the Mackenzie Shelf region
10  between 18 July and 22 August 2009 during the successive ArcticNet and Malina campaigns that took place on board the research icebreaker CCGS *Amundsen* (Fig. 1, Appendix A). The first leg (16–29 July) was a component of the annual expedition of the ArcticNet Network aiming to assess ecosystem dynamics in coastal waters of the Canadian Arctic. The second leg (30 July–27 August) was led by the Malina project,
15  which covered the Mackenzie Shelf region with a comprehensive sampling grid primarily composed of 7 shelf-basin transects (Fig. 1). The data collected over ArcticNet-Malina was divided according to bottom depth in order to investigate the mean inshore-offshore gradients in total particle concentration, zooplankton abundance, as well as associated volume/biomass and size distribution. The shelf, slope and basin regions
20  were defined as the sampling stations located within the < 100 m, 100–1000 m and > 1000 m isobaths, respectively. This grouping enabled us to evaluate the large-scale variations and to process the CTD, UVP5 and net tow datasets on the basis of an independent variable.

## 2.2  Underwater Vision Profiler, CTD-rosette casts and image processing

25  The Underwater Vision Profiler 5 (UVP5) is a compact and autonomous underwater imaging system developed and initially constructed at the Laboratoire d'Océanographie de Villefranche-sur-Mer (LOV) located in Southern France. The instrument is now

manufactured by HydroptiC (http://www.hydroptic.com/) in collaboration with the LOV. Full details of the technical specifications and processing operations of the UVP5 can be found in Picheral et al. (2010).

The UVP5 used in the present study was designed to be a component of the rosette profiler equipped with a conductivity-temperature-depth system (CTD, Seabird SBE-911+) and was deployed on a routine basis throughout the campaign (Fig. 1). Most CTD/UVP-rosette vertical profiles were conducted over the whole water column, i.e. from 10 m above seafloor up to the surface (see Appendix A for the list of stations). A fluorometer (Seapoint chlorophyll fluorometer) and a transmissometer (WET Labs C-Star 25 cm) were also connected to the CTD system. The CTD data were calibrated and verified following the Unesco Technical Papers (Crease, 1988). Water samples were taken on board for salinity calibration using a Guildline Autosal salinometer (resolution $< 0.0002$, precision $\pm 0.002$). Fluorescence data from the fluorometer were post-calibrated against in situ chlorophyll-$a$ (chl-$a$) concentrations. Validated data from all CTD casts were averaged over 5-m bins using a centered moving average.

During deployment, the UVP5 recorded and measured all objects $> 100\,\mu$m in real time (i.e. both non-living particles and zooplankton). Images of all particles were recorded at a frequency up to 5.5 Hz, corresponding to a distance of $\sim 20$ cm between images at the $\sim 1$ m s$^{-1}$ lowering speed of the CTD-rosette profiler. The recorded volume per image was 1.02 l and the conversion equation from pixel area to size was $S_\mathrm{m} = 0.003 S_\mathrm{p}^{1.3348}$, where $S_\mathrm{m}$ is the surface in mm$^2$ and $S_\mathrm{p}$ the particle area in number of pixels (Picheral et al., 2010). The real time processing was set to a mixed process mode. The size and grey level of every object $> 100\,\mu$m were calculated in situ, but only images of all large objects $> 600\,\mu$m were backed up on a memory stick for further analysis. When the UVP5 was back on the ship deck, both the complete dataset of total particles and the logged images of objects $> 600\,\mu$m were transferred on a computer for complete analysis. The size spectra of total particle abundance and volume were computed at an interval of 5 m. Images of all objects $> 600\,\mu$m were processed using the Zooprocess imaging software (http://www.zooscan.com) in order to calculate

Title Page

Abstract | Introduction

Conclusions | References

Tables | Figures

|◀ | ▶|

◀ | ▶

Back | Close

Full Screen / Esc

Printer-friendly Version

Interactive Discussion

40 geometric and grey-level variables to identify major zooplankton by the freeware Plankton Identifier (PkID) based on Tanagra data mining and implemented as part of the Zooprocess package (see Gorsky et al., 2010 for details). The prediction of organisms obtained from the PkID files was exhaustively post-validated by experts to obtain an accurate dataset of abundance and biovolume for zooplankton larger than 600 μm.

The size distributions of the abundance and volume of total particles and zooplankton recorded at each station were normalized according to the interval of each size-class (Platt and Denman, 1978). This dataset was then divided and averaged for the shelf ($< 100$ m isobath), slope ($100$–$1000$ m) and basin ($> 1000$) regions to provide a more comprehensive overview of particle dynamics and large-scale spatial trends across the inshore-offshore interface (Fig. 1, Appendix A). The relationship between the abundance/volume and the size of particles/zooplankton was approximated by the two-parameter power-law equation $n = bd^k$, where $n$ is the normalized particle abundance or volume, $b$ a constant, $k$ the scaling exponent (slope in a log-log form) and $d$ the equivalent spherical diameter (ESD) of a given particle or organism (also referred as apparent diameter, see Stemmann and Boss, 2012 for further details).

## 2.3 Zooplankton net tows, traditional taxonomic counts and ZooScan measurements

Zooplankton assemblage integrated over the entire water column was collected using a quadruple 1-m$^2$ metal frame sampler equipped with flowmeters and plankton nets of 200 μm mesh size (Darnis et al., 2008). At each station (see Appendix A), the sampling gear was deployed vertically from 10 m above the bottom up to the surface at a speed of 45 m min$^{-1}$. Zooplankton samples were condensed and preserved in seawater solution poisoned with borax-buffered 4 % formalin for further analysis. Preserved samples were divided in two distinct fractions in order to proceed to: (1) manual taxonomic counts; and (2) sample digitization and analysis using a ZooScan (Gorsky et al., 2010). Traditional taxonomy and validation of random ZooScan vignettes were performed at Laval University (Québec, Canada), whereas ZooScan digitization and

**Particles and zooplankton in Beaufort Sea**

A. Forest et al.

Title Page

| Abstract | Introduction |
| Conclusions | References |
| Tables | Figures |

|◄ | ►|
◄ | ►

Back | Close

Full Screen / Esc

Printer-friendly Version

Interactive Discussion

image post-processing with the Zooprocess software were made at LOV (Villefranche-sur-Mer, France).

Subsamples for manual taxonomy were rinsed with freshwater and sieved through 1000 and 150 µm meshes to separate large and small organisms. The two size frac-
tions (< 1000 µm and > 1000 µm) were divided with a Motoda-type splitting box and known aliquots were resuspended in distilled water. From each sub-sample, approximately 300 zooplankton organisms were enumerated in a Bogorov counting tray and identified to the lowest possible taxonomical level. The Arctic copepod species *Calanus glacialis* and the Pacific Subarctic *C. marshallae* that may co-occur in the region (Frost,
1974) were pooled into a single taxon due to lack of certainty in their differentiation (Darnis et al., 2008).

Subsamples for ZooScan analyses were also divided with a Motoda splitter, resuspended in distilled water and fractionated to obtain two size-fractions (< 1000 µm and > 1000 µm). Each size-fractionated sample was gently poured in a 15 × 24 cm Plex-
iglas tray on the scanner (2400 dpi resolution). Prior to digitization, manual separation of plankton organisms with fine tweezers was performed directly into the tray to avoid multiple objects to be treated as one. In some cases, separation of objects was also performed computationally after digitization. Scanned samples were normalized using the full spectrum of grey and a blank (i.e. scan without objects) was
subtracted from each image. The Zooprocess software was used to extract and measure every object detected in images produced by the ZooScan (pixel resolution of 10.6 µm). The major and minor axis of the best fitting ellipse for each object were measured and an equivalent apparent elliptical biovolume (EBv) was estimated as: $EBv = 4/3 \cdot \pi \cdot (major/2) \cdot (minor/2)^2$. Many other variables (Appendix 4 in Gorsky et al.,
2010) were also used for the automatic classification of objects. The automatic recognition of zooplankton was performed using the free software PkID as mentioned in Sect. 2.2. The training set for ZooScan consisted of 2100 validated vignettes of random objects (including detritus). This algorithm was used to classify organisms from the net tow samples in major zooplankton groups. The copepods were successfully recognized

A. Forest et al.

Full Screen / Esc

Printer-friendly Version

Interactive Discussion

(true positive = 84.9 %, contamination = 19.4 %) while appendicularians were less recognized (true positive = 66.7 %, contamination = 32.9 %) (Table 1). The automatic prediction was further corrected by a manual validation to ensure accurate estimate of zooplankton groups.

For comparisons with the UVP and ZooScan biovolume datasets, the abundance of copepods (copepodites only, including adults) obtained from manual counts was converted into volume units by assimilating the body shape of a copepod to an ellipsoid for the prosome and to a cylinder for the urosome (Mauchline, 1998). Biovolume estimates based on the ellipsoid-cylinder combination were further corrected for body parts not taken into account by this method (e.g. legs, furca, antennae) using a correction factor of 1.2–1.7 depending on the average areal ratio of the supplementary parts to the mean prosome and/or urosome area. Mean lengths, widths and ratios of body parts of Arctic copepods were obtained from the historical collection of copepod measurements from the taxonomic laboratory of L. Fortier (Laval University, Canada). Missing measurements were gathered from the global literature, as cited in the online databases of Razouls et al. (2005–2011) and Appeltans et al. (2011). No morphometric estimates were attempted on zooplankton else than copepods due to uncertainties on the average body measurements of the other groups.

The size distributions and power-law relationships between abundance/biovolume and size of zooplankton from the vertical net tow datasets (i.e. ZooScan and manual counts/morphometric estimates) were calculated the same way as for the UVP5 dataset (see previous section).

**Particles and zooplankton in Beaufort Sea**

A. Forest et al.

Title Page

Abstract | Introduction

Conclusions | References

Tables | Figures

◄ | ►

◄ | ►

Back | Close

Full Screen / Esc

Printer-friendly Version

Interactive Discussion

# 3 Results

## 3.1 Underwater Vision Profiler: magnitude and distribution of particles and zooplankton across the Mackenzie Shelf in late summer 2009

Mean total particle ($> 100\,\mu$m) abundance and volume recorded with the UVP5 in the surface layer ($\geq 50$ m) of Southeast Beaufort Sea in July/August 2009 exhibited a decline of ca. 2 orders of magnitude when progressing from the shelf toward the basin (Fig. 2a,c). Over the shelf, maximum and minimum particle concentrations were observed around 40–50 m and 60–65 m depth, respectively (Fig. 2a). Maximum and minimum particle volumes across the three regions (Fig. 2c) corresponded roughly to patterns in total particle abundance (Fig. 2a) and in chl-*a* (Fig. 2e). Mean chl-*a* concentration over the shelf was low ($\sim 1.5$ mg chl-*a* m$^{-3}$ in the SCM between 30–50 m), but remained higher than values measured for the slope and basin regions ($\sim 0.3$ mg chl-*a* m$^{-3}$ between 50 and 80 m) (Fig. 2e). Mean chl-*a* concentration and beam attenuation coefficient were also relatively high in the top 10 m over the shelf (Fig. 2e,f). Maximum abundance and biovolume of zooplankton were detected between 30 and 70 m depth (Fig. 2b,d). This interval appears to correspond to the most active water layer in terms of total particle concentration and primary production during the study period.

The spike-like increase in particle abundance just below 70 m on the shelf (Fig. 2a) was symptomatic of a widespread benthic nepheloid layer (BNL) comprised of small particles (Fig. 2c). The presence of a BNL over the shelf was supported by the slight increase of beam attenuation coefficient around 70–75 m depth (Fig. 2f). Mean particle abundance and volume over the slope peaked around 40–50 m. While total particle abundance was relatively stable throughout the water column over the slope, particle volume decreases rapidly with increasing depth past its maximum (Fig. 2a,c). Contrastingly, particle abundance increased with increasing depth in the basin region (Fig. 2a), whereas volume in this area did not vary much (Fig. 2c).

The fit of a power-law model to the measured particle size distribution (calculated using the full ESD range of 0.1–12 mm) was statistically significant both for the abundance

Title Page

Abstract | Introduction

Conclusions | References

Tables | Figures

◀◀ | ▶▶

◀ | ▶

Back | Close

Full Screen / Esc

Printer-friendly Version

Interactive Discussion

($r^2 = 0.99$, $p < 0.0001$) and volume ($r^2 = 0.66$–$0.79$, $p < 0.0001$) spectra (Fig. 3). Overall, the power-law fits were less robust for the volume size-spectra than for the abundance spectra. The exponent ($k$) of the normalized size spectra of total particle abundance and particle volume remained relatively similar, whereas $k$ values in the size
5 distribution of zooplankton abundance and biovolume both decreased with increasing distance from shore (Fig. 3). Zooplankton abundance and biovolume estimated with the UVP5 decreased, respectively, from $\sim 84$ to $\sim 9$ individuals (ind.) $m^{-3}$ and from $\sim 2.5$ to $\sim 0.1\, cm^3\, m^{-3}$ across the inshore-offshore gradient (Table 2). Such values were likely minimum estimates as zooplankton $\leq 1$ mm ESD were not accurately quan-
10 tified by the UVP5, as seen in Fig. 3. Accordingly, the power-law model was fitted to the zooplankton size spectra only for organisms $> 1$ mm ESD. The power-law equations presented in Fig. 3 enabled us to calculate the idealized contributions of planktonic particles to the total particle inventory in each size-class of the full ESD range of 0.1–12 mm (Fig. 4). These estimations revealed that living particles accounted for an
15 increasingly large proportion of total particles from the shelf to the basin (e.g. $< 1\%$ over the shelf vs. $\sim 15\%$ in the basin for particles $< 1$ mm) and as the size of particles was increasing (up to $\sim 55\%$ for 12 mm particles in the basin) (Fig. 4).

The zooplankton identified with the UVP5 comprised 6 major groups: protozoans, copepods, appendicularians (i.e. bodies and houses), chaetognaths, ctenophores,
20 and other gelatinous organisms (Fig. 5, Table 2). A last category included objects ($> 600$ µm) that could have been zooplankton, but that could not be recognized with confidence. These objects were grouped as unidentified particles and contained both detrital aggregates and living organisms. Copepods dominated numerically (82–84 %) the total zooplankton assemblage across the 3 regions (Table 2). Copepods were
25 found in all size classes from 0.7 to 10 mm and dominated the total abundance and biovolume up to an ESD size of 5–6 mm (Fig. 6). The total biovolume was, however, dominated by appendicularians over the shelf and slope (58–71 %, Table 2), mainly because substantial amounts of large appendicularians houses (7–12 mm ESD) were detected at all depths by the UVP5 throughout the area (Fig. 5). It should be noted

Title Page

Abstract | Introduction

Conclusions | References

Tables | Figures

◄ | ►

◄ | ►

Back | Close

Full Screen / Esc

Printer-friendly Version

Interactive Discussion

that a fraction of these houses could be old discarded houses, so uncertainties remain regarding the actual contribution of living appendicularians to total biovolume. Even if not dominating, appendicularians represented also a substantial fraction (28 %) of zooplankton biovolume in the basin (Table 2).

Vertical distribution of zooplankton, as recorded with the UVP5, varied markedly among groups and regions (Fig. 5). Over the shelf, protozoans and chaetognaths decreased with increasing depth, whereas other groups generally showed an inverse pattern. Copepods exhibited maximum abundance and biovolume in the interval 50–75 m, just below the SCM that occupied the 30–50 m layer over the shelf (Fig. 2e). Except for ctenophores, zooplankton concentration was overall low near the bottom (75–100 m) of the outer shelf (Fig. 5). Almost no ctenophore was detected beyond the shelf margin (Fig. 5e,k). Over the slope, protozoans showed maximum concentration near the shelf break around 100–300 m (Fig. 5a,g). Copepods and appendicularians over the slope were densest in the interval 25–100 m. In the basin, appendicularian biovolume increased with depth in the top 100 m and exhibited a peak in the 75–100 m layer (Fig. 5i). Chaetognath abundance was well distributed throughout the water column over the slope (Fig. 5c), but its marked biovolume increase in the deep Atlantic layer ($\sim$ 300–1000 m, Fig. 5j) suggested the presence of particularly large organisms in that layer (up to 10 mm ESD, Fig. 6b,e). In the basin, zooplankton abundance and biovolume of copepods and protozoans were generally similar than over the slope, while other groups were much lower (Figs. 5, 6). Appendicularians, ctenophores and other gelatinous dominated the upper size range (Fig. 6). Surprisingly, protozoans were identified up to a size class of 2–3 mm (Fig. 6), suggesting the presence of large unicellular organisms throughout the study area, such as radiolarians and foraminifera.

## 3.2 Vertical net tows: composition of the zooplankton assemblage and comparisons with the overlapping stations from the UVP dataset

A total of 93 zooplankton taxa were identified by traditional taxonomic counts in the collection of samples from the 200-µm mesh nets deployed across the Mackenzie

Shelf in July/August 2009 (Fig. 1, Appendix A). These zooplankton taxa were classified in large groups (Table 2) in order to provide a resolution similar to that of the UVP5 dataset (Table 3). Across the shelf, slope and basin regions, copepods (i.e. nauplii and copepodites, the latter including adults) represented 77.6 %, 94.1 % and 92.4 % by numbers of all the organisms collected, respectively (Table 3). The ratio of nauplii-to-copepodites was highest over the shelf (0.32) and relatively low over the slope (0.08) and in the basin (0.06). Nauplii could be identified only to the genus level, which revealed that ∼ 75 % of the community of nauplii > 200 µm was (unsurprisingly) comprised of *Calanus* spp. (data not shown). The copepodite assemblage (including adults) was dominated by a guild of ten taxa representing ∼ 95 % of all the copepodites collected (Fig. 7a). The small *Oithona similis* was the most abundant species (∼ 26–30 % of the assemblage) across the 3 regions, but *Pseudocalanus* spp. contributed an equivalent fraction (∼ 30 %) over the shelf while representing a minor component (∼ 6–7 %) in the slope and basin assemblages. By contrast, increasing proportions of *Oncaea* spp. and *Spinocalanus* spp. (both from < 1 % to ∼ 12 %) and *Microcalanus* spp. (from ∼ 9 % to ∼ 21 %) were detected across the inshore-offshore gradient.

The approximative ESD of the most abundant copepod species present in the Southeast Beaufort Sea spanned from ∼ 0.3 up to ∼ 7 mm (Fig. 8). The mean biovolume of the total copepodite assemblage (including adults) across the shelf, slope and basin regions decreased exponentially with increasing distance from shore (Table 3). As expected, the biovolume was dominated by the large calanoid species *Calanus hyperboreus* (∼ 51–58 %) and *C*. *glacialis* (∼ 14–31 %) (Fig. 7b). The medium-sized *Metridia longa* accounted for a relatively low proportion of the biovolume on the slope and in the basin (∼ 9–12 %) and was quasi-absent over the shelf (∼ 1 %). Similarly, the large *Paraeuchaeta glacialis* represented an increasingly important proportion (from ∼ 4 % to ∼ 12 %) of the biovolume from the shelf to the basin.

The regional automatic recognition algorithm developed for ZooScan analyses enabled us to classify zooplankton from the net tow samples in 3 major groups: copepod (copepodites, including adults), appendicularians and carnivorous gelatinous (Table 4).

The latter group comprised chaetognaths and medusae-like organisms that represented a relatively minor proportion of the total zooplankton identified by the ZooScan algorithm. A fourth category for detritus was also created because the net tow samples often contained a fair amount of detrital matter (Table 1). Results for the total copepod assemblage from the ZooScan analyses showed general consistency with the ones resulting from manual counts (Tables 3, 4). The only noticeable difference was the biovolume estimated for the basin region, which was more than twice higher in ZooScan analyses than from morphometric estimates of manual counts.

For the overlapping stations (Fig. 1), the regional averages of the size distributions of copepod biovolume and abundance, as evaluated via the 3 methodologies (manual estimates, ZooScan and UVP5), showed coherent patterns co-varying in the same order of magnitude over the size-spectrum of 1–6 mm (Fig. 9). However, the loss of efficiency in detection of the UVP5 in the lower size-spectrum (Fig. 3) prevented the reliable quantification of organisms less than $\sim 1.0$ mm ESD, whereas the ZooScan and manual estimates did quantify satisfactorily copepods down to $\sim 0.4$ mm ESD. Every method showed an apparent maximum limit of detection around $\sim 6$ mm ESD (Fig. 9), indicating that both the net tows and the UVP5 quantified reliably the same size-classes in the upper size spectrum ($\geq 1$ mm ESD). Accordingly, we calculated the parameters of the power-law equations ($n = bd^k$) from the normalized copepod size distributions with the pooled datasets obtained from the 3 methods within the size-ranges where the quantification was adequate (i.e. 0.4–6 mm for net tow estimates and 1–6 mm for UVP5 estimates). This approach revealed that the size-spectrum slopes of both copepod abundance and biovolume gradually decreased across the shelf-basin interface (Fig. 9). Within the size-range of 1–6 mm ESD, where no loss of efficiency in detection was observed, all 3 methods provided statistically correlated distributions ($0.91 > r^2 > 0.60$, $0.0001 < p < 0.01$, Pearson's Model II Regression) within a proportional ratio close to 1 : 1 ($1.09 \pm 0.49$). Based on manual counts and ZooScan analyses, the abundance of copepods $< 1$ mm ESD accounted for a substantial proportion of total abundance ($\sim 77$–$89\,\%$), but the biovolume was overwhelmingly dominated

(~ 93–97 %) by copepods > 1 mm ESD (Fig. 9). When integrated over the size-range of 1–6 mm, the log-transformed mean abundance and biovolume of copepods estimated at each overlapping station (Fig. 1, Appendix A) with the 3 different methods showed relatively robust associations ($0.94 > r^2 > 0.64$) and significant similarities (slope close to ~ 1, all at $p < 0.01$) (Fig. 10).

## 4 Discussion

### 4.1 Environmental context and regional variability in the abundance, volume and size distribution of particles and mesozooplankton

Despite the fact that the Mackenzie Shelf region is affected by a substantial load of fluvial sediment (Macdonald and Yu, 2006), no particular maximum in the total particle concentration was noticed near the ocean surface in the present study. Instead, the main peak in particle concentration was linked to the occurrence of a widespread subsurface chlorophyll maximum (SCM; Martin et al., 2010) detected across the region between 30 and 70 m depth. The rather low background of particulate matter present down to ~ 30 m supports that most terrigenous particles carried by the Mackenzie River sink near the coast (~ 97 % of total mass; O'Brien et al., 2006). The only apparent signature of the river plume was detected in the beam attenuation coefficient and chl-*a* profiles whose the signals showed visible rise above ~ 10 m (Fig. 2e,f). Such a vertical pattern near the surface was the likely result of riverine waters expanding over the shelf (cf. Carmack and Macdonald, 2002) that sustained some phytoplankton biomass (~ 0.6 mg chl-*a* m$^{-3}$) and contained small particles of the size-class ~ 0.5–20 µm – to which the beam attenuation coefficient is sensitive (Boss et al., 2001 and references therein). The fine particles that accumulated in the stratified surface layer were presumably a mixture of clay-silt material and fresh algae (cf. O'Brien et al., 2006). By contrast, the relatively high chl-*a* signal (~ 1.5 mg chl-*a* m$^{-3}$) recorded at depth suggests that phytoplankton biomass was primarily fuelled by subsurface nutrients. The

magnitude and positioning of the chl-*a* maximum indicate that the phytoplankton bloom in late-July/August 2009 in Southeast Beaufort Sea was "matter of the past", as they compared well with the configuration observed toward the end of summers 2004 and 2008 (Tremblay et al., 2008; Forest et al., 2011). In fact, except for few shallow sta-
tions located over the shelf, nitrate was exhausted in the upper $\sim 40$ m across the study area and primary production was relatively low, averaging $45 \pm 25$ mg C m$^{-2}$ d$^{-1}$ in late summer 2009 (P. Raimbault and N. Garcia, LMGEM, France, unpublished data). Nevertheless, the integrated chl-*a* biomass in the upper water column was roughly 4-folds higher over the shelf than beyond stations of depth $> 100$ m (Fig. 2). Nitrate is the ul-
timate limiting factor of primary production in the Beaufort Sea (Tremblay et al., 2008), but this does not exclude a posteriori that the presence of sea ice across the slope and basin regions could have been a local property that restrained phytoplankton growth offshore by limiting light available at the nitracline (Carmack et al., 2004; Martin et al., 2010). Actually, unusually high concentrations of old sea ice from the Central Arctic
pack were pushed southward in the Beaufort Sea in July 2009 by persistent northerly winds (CIS, 2009). The Mackenzie Shelf was generally free of ice over our sampling period, while sea ice remained abnormally close to the shelf margin located $\sim 100$ km north off the Tuktoyaktuk Peninsula.

Overall, zooplankton populations (as estimated with the UVP5) mirrored the inshore-
offshore patterns of chl-*a* and total particle volume. The proportion of zooplankton relative to non-living particles increased with greater distance from shore and as the ESD of particles was increasing. These observations suggest that the ratio of plankton to total particles $< 1$ mm ranged from less than 1 % on the shelf to $\sim 5$–15 % offshore. Then, the living fraction got rapidly more important for sizes above $\sim 1$ mm, so that
non-living particles would represent $< 50$ % of total particle inventory around 1–2 cm and should be virtually absent in size-classes over 4–5 cm (based on Fig. 4). The relatively high proportion of zooplankton vs. non-living particles in the basin compared with the shelf is in agreement with Olli et al. (2007) who observed that heterotrophs are numerous relative to phyto-detritus and marine snow in the central Arctic basins.

As in other oceans, most of large sinking particles in the Arctic Ocean probably settle over the continental shelf (Ashjian et al., 2005) while a strong grazing pressure offshore leaves little fresh biomass available for vertical export (Olli et al., 2007). Furthermore, the fraction of small organisms in the total plankton assemblage was increasing from the shelf to the basin since the slopes of the biovolume and abundance size-spectra were gradually more negative (Fig. 3). Although we cannot confirm that the fits derived from the UVP5 dataset were representative of the lower size range (< 100 µm), they are consistent with the view that small plankton communities are a preponderant feature of the Canada Basin (Li et al., 2009; Kosobokova and Hopcroft, 2010) as well as of most deep oceanic biomes (Richardson and Jackson, 2007). A food web based on small plankton might lead to more recycling and less export of organic matter to depth or up in the food chain. By contrast, we can deduce that the shelf was more favorable to large planktonic species, and thus, to more energy transfer to higher trophic levels (e.g., Frangoulis et al., 2010). However, such a simplistic distinction of the function of a given food web can be debated, since size alone is not always a direct proxy for export or retention pathway (Richardson and Jackson, 2007). Also, our study has been conducted over a limited spatial-temporal window (36 days), during a heavy ice year and toward the end of the productive season. So it is difficult to conclude on the functioning of the ecosystem in the context of an apparent quiescent period in terms of biological activity.

Nevertheless, the high-resolution CTD-UVP5 profiles conducted across the Mackenzie Shelf in late summer 2009 showed that zooplankton might have exerted an important grazing pressure on phytoplankton biomass. The vertical distribution patterns of zooplankton generally co-varied with chl-*a* concentration, a well-known feature of the world's oceans (e.g., Longhurst, 1985). However, several differences in the vertical and regional distribution patterns were observed between the specific zooplankton groups (Fig. 5). Copepods (representing ∼ 83 % of the total quantity of zooplankton identified by the UVP5) showed maximum abundance and biovolume between 50–75 m throughout the 3 regions. This interval corresponded to the water layer located just below the

**Particles and zooplankton in Beaufort Sea**

A. Forest et al.

Title Page

Abstract | Introduction

Conclusions | References

Tables | Figures

◀ | ▶

◀ | ▶

Back | Close

Full Screen / Esc

Printer-friendly Version

Interactive Discussion

SCM over the shelf, whereas it was associated with the weak chl-*a* signal offshore. Interestingly, the maximum in total zooplankton abundance (mostly copepods) on the shelf was located at ∼ 55 m depth, a few meters underneath the chlorophyll/particle-rich layer (Fig. 2). At this depth, a marked negative anomaly in the size-spectrum of non-zooplankton particles was observed between 0.7 and 4 mm ESD (down to 4 times less than expected around 1.5 mm, not shown). These results support the conclusion of Jackson and Checkley (2011) that the base of the particle-rich layer is a zone of intense particle consumption where zooplankton might act as "gatekeepers" for the vertical export of organic matter. Copepods indeed play a key role in the Arctic marine food web as one of the main regulators of vertical particle fluxes (Wassmann et al., 2003; Wexels Riser et al., 2008; Forest et al., 2011). In the Beaufort Sea, copepods may thus act as a node in the channel of organic matter by grazing within the SCM and from its underside.

Due to the secretion of large mucous filter-houses (> 7 mm ESD), appendicularians accounted for a substantial proportion (∼ 28–69 %) of the total zooplankton biovolume across the shelf-basin interface. Appendicularians were concentrated between 25 and 50 m depth, just above or within the layer occupied by the SCM, suggesting intense agglomeration of fine particles (∼ 0.2–30 μm; Deibel, 1998) into gel-like aggregates at these depths. Interestingly, the volume occupied by large appendicularian houses was increasing with depth until 100 m in the basin region (Fig. 5i). This implies that a fraction (∼ 10–25 %) of the larvacean houses produced on the shelf and slope was probably exported offshore. However, appendicularian biovolume was almost at nil values below 100 m depth beyond the shelf break (Fig. 5i), indicative of disaggregation and recycling of carbon-rich discarded larvacean houses (Alldredge, 1976) occurring in the Pacific Halocline. The relatively high concentration of protozoans in waters between 75 and 300 m depth in the slope and basin regions (Fig. 5a,g) may be the sign of an important detrital processing chain prevailing in this water mass offshore. Large suspension-feeding protozoans, such as foraminifera and radiolarians, which feed opportunistically on detritus, gels and bacteria (Capriulo, 1990), are potentially good candidates

to explain the occurrence of such a detritus-based food web below the euphotic zone. The off-shelf advection of particulate matter from the shelf sediment is also a potential mechanism for sustaining an active detrital pathway in intermediate waters around the Mackenzie Shelf in the Southeast Beaufort Sea (Forest et al., 2008). Indeed, in both the slope and basin areas, the weak indentation in total particle abundance around 100 m depth was likely symptomatic of mild intermediate nepheloid layers of fine particles originating from the shelf and propagating offshore at the depth of the shelf break (Fig. 2a,c). The increasing relative proportion of large carnivores in the mesopelagic zone (i.e. chaetognaths and other gelatinous organisms compared with copepods and appendicularians) is another evidence that supports the prevalence of a multivorous network at depth (e.g., Longhurst, 1985, Stemmann et al., 2008). Finally, the absence of most zooplankton groups below 1000 m (Fig. 5) suggests a "diluted" food web in the deep Canada basin, as also observed by Kosobokova and Hopcroft (2010).

## 4.2 Contrasting results of the zooplankton community structure as observed with the Underwater Vision Profiler and vertical net tows

Matching results from zooplankton net tows to those of video profilers is a challenge that can be hardly overcome due to fundamental differences in their acquisition method (e.g., Remsen et al., 2004) and/or to the fact that spatial distribution of plankton is patchy at various scales (Folt and Burns, 1999). In the present study, both the UVP5 and net tow datasets revealed that copepods were the most abundant groups, but marked discrepancies could be noticed in the absolute values presented in Tables 2–4. Total copepods (i.e. nauplii and copepodites, including adults) were systematically 2–5 times higher in counts from net tow samples than from the UVP5. This divergence was obviously linked to the methodology and it is thus important to understand the limitations of each sampling gear before comparing the datasets. The towing speed of nets and UVP5 was relatively similar (45–60 m min$^{-1}$), but zooplankton avoidance of the descendent rosette profiler cannot be excluded. However, the UVP5 is equipped with a red light system in order to reduce zooplankton phototactic behavior (Picheral

et al., 2010). Hence, the difference in copepod abundance was presumably mainly due to the fact that the UVP5 did not estimate reliably the quantity of zooplankton < 1 mm close to the size limit of detection (Fig. 3) and that nauplii could not be identified due to their small size (< 600 µm). Over the shelf, the abundance of appendicularians was also ∼ 6 times higher based on net tow sampling than with the UVP5, but the associated error was also high (Table 3). This result was unexpected in the sense that it is commonly known that traditional net tows cannot provide reliable estimates of fragile organisms such as appendicularians. On the one hand, a large fraction of appendicularians over the shelf could have been less than ∼ 1 mm ESD. Such hypothesis is quite plausible since appendicularians in the surface layer of Arctic seas (mainly oikopleurids) typically average 0.26 mm length and show an inverse relationship between body size and abundance (Deibel and Daly, 2007). Due to their elongated "tadpole" body shape, small appendicularians could get caught by 200-µm mesh size nets without being identified by the UVP5. On the other hand, a patchy appendicularian swarm might have simply been sampled by one of the net tows conducted over the Mackenzie Shelf. Actually, a high number (> 5000) of small bodies of *Oikopleura* spp. (< 1 mm length) were found in the net tow sample from the first shallow station (∼ 60 m), which has not been recorded in the UVP5 profile conducted a few hours later at that same location. This observation reinforces the fact that both methodological differences and spatial patchiness should be considered when interpreting zooplankton data from net tows and video profilers.

The abundances of chaetognaths and protozoans estimated by both the vertical net tows and the UVP5 were low but similar (Tables 2, 3), suggesting that both approaches provided an adequate resolution of these two zooplankton groups. Protozoans identified in the net tow samples were composed exclusively of radiolarians and foraminifera, two amoeboid-like plankton that could comprised species > 600 µm and/or form colonies, which would explain their occurrence in the UVP5 dataset. This planktonic group seems to be a ubiquitous inhabitant of the mesopelagic layer as observed across 9 marine biogeochemical provinces (Stemmann et al., 2008). Such findings

highlight that protozoans are not only members of the microzooplankton size-class < 200 µm (Calbet et al., 2008), but also important members of the mesozooplankton – thus potentially playing an unsuspected role in the "intermediate" food web. Some zooplankton groups found in the net tow samples were not identified by the UVP5 and vice-versa (Tables 2, 3). For example, pteropods and ostracods were not reported by the UVP5, a weakness that needs to be corrected for future studies since these two groups can be at time important components of the Arctic marine ecosystem (Forest et al., 2011). Although here, they were apparently minor contributors to the zooplankton assemblage. Patchy spatial distributions of those groups may also be responsible for the discrepancies between the two datasets. Furthermore, it is possible that the ctenophores identified by the UVP5 were in fact cnidarians, as no ctenophore was found in net tow samples. However, small comb jellies (and other fragile gelatinous organisms) could have been destroyed when towing the net in the water column, whereas larger medusae such as cnidarians (> 1–2 cm) might have resisted the ascent while not being resolved by the camera.

If we go beyond the main divergences between the UVP5 and net tow datasets, the information obtained when combining the two methods is actually complementary and instructive. The UVP5 enabled high spatial resolution and the recognition of fragile organisms, whereas the net tows provided high taxonomic resolution and the collection of more groups than the camera profiler was able to identify (e.g. pteropods). General patterns in the mesozooplankton community structure were also consistent between methods. In particular, all 3 methodologies (manual, ZooScan and UVP5) delivered consistent estimates of copepod biovolume (Tables 2–4), which demonstrates that copepod biomass is overall driven by large organisms (cf. Darnis et al., 2008). With an efficient resolution of the size-range ∼ 1–6 mm ESD for copepods (Fig. 9), the UVP5 appeared to have captured adequately the bulk biomass of the dominant calanoid copepods in terms of total biomass (i.e. *C. hyperboreus*, *C. glacialis* and *M. longa*; Fig. 8) that are of utmost importance for trophic transfer in the Beaufort Sea (Forest et al., 2011). In fact, the abundance and biovolume of copepods estimated at each

**Particles and zooplankton in Beaufort Sea**

A. Forest et al.

Title Page

Abstract | Introduction

Conclusions | References

Tables | Figures

|◄ | ►|

◄ | ►

Back | Close

Full Screen / Esc

Printer-friendly Version

Interactive Discussion

station within the size-range of 1–6 mm was generally coherent even if the technical approach was different (Fig. 10). The significant inter-method relationships of copepod biovolume and abundance were robust ($0.94 > r^2 > 0.64$), which gave us confidence that the UVP5 dataset was representative of the assemblages of large copepods collected by the net tows. However, the small copepods < 1 mm ESD that accounted for a substantial proportion of the abundance ($\sim 77$–89 %) obtained through net tow sampling were not efficiently identified (if not at all) by the UVP5. Still, this underscores the need of conducting traditional sampling if the determination of the fine structure of the zooplankton assemblage is the goal of a given study. But if the pursued objective is to rapidly get reliable estimates of total copepod biomass, the UVP5 appears to be a convenient approach. Therefore, we can relate the biovolume of Arctic copepods that occupy the size-range of $\sim 1$–6 mm ESD to their carbon content, as estimated with regional carbon-prosome length equations (see Forest et al., 2011). This produces a general biovolume-to-carbon conversion factor that can be used to estimate copepod biomass with the UVP5 in Arctic waters. This relationship is presented in Fig. 11.

The detailed composition of the zooplankton assemblage obtained with manual taxonomic counts in the present study supports generally what we know of the diversity and distribution of mesozooplankton in the Arctic Ocean. Apart from the classical notions that plankton biodiversity is relatively low (Table 2) and that copepod biomass is dominated by large calanoids (Fig. 7), some observations can, however, be made. Above all, the shelf environment was obviously the most active region in terms of herbivorous feeding and reproduction activities, and probably for the trophic transfer of organic matter too (as suggested in Sect. 4.1). First, the two large herbivores *C. hyperboreus* and *C. glacialis* that constitute key energy links in the Arctic food web (Falk-Petersen et al., 2009) represented alone $\sim 89$ % of the total copepod biomass over the shelf. Second, the small-sized *Pseudocalanus* spp. (which is the main prey of young stages of Polar cod, the dominant fish in the Arctic) was most abundant over the shelf, accounting for $\sim 30$ % by number of the total copepodite assemblage (cf. Darnis et al., 2008). Third, roughly 90 % of all copepod nauplii (*Calanus* spp. at $\sim 75$ %) collected by

**Particles and zooplankton in Beaufort Sea**

A. Forest et al.

Title Page

Abstract | Introduction

Conclusions | References

Tables | Figures

|◄ | ►|

◄ | ►

Back | Close

Full Screen / Esc

Printer-friendly Version

Interactive Discussion

the 200-μm mesh nets were found at stations < 100 m bottom depth. By contrast, the offshore assemblage was increasingly composed of carnivores, omnivores and detritivores species. For example, the large carnivore *P. glacialis* represented a gradually large proportion (4 % to 12 %) of the copepod biomass when progressing from the shelf toward the basin. Also, the well-known omnivore *M. longa* (e.g., Sampei et al., 2009) was almost absent over the shelf, but accounted for ∼ 9–12 % of the total copepod biomass in the two other regions. Furthermore, the small detritivore *Spinocalanus* spp., which is physiologically engineered to digest refractory detrital matter (Kosobokova et al., 2002), was the 5th most important species in terms of biomass beyond the shelf break. Due to their small ESD size (Fig. 8), the two latter species were likely responsible for the more negative $k$ values (spectrum slopes) of copepod abundance and biovolume recorded across the shelf-basin interface (Fig. 9), a trend comparable to what has been detected in the total zooplankton size distributions (Fig. 3). Therefore, the net tow dataset supported our previous assumption of the increasing prevalence of a high-recycling, low-productive and presumably low-export food web with increasing distance from the ice-free shallow region of Southeast Beaufort Sea in late summer 2009.

## 5 Conclusions

Over the Mackenzie Shelf in late summer 2009, the average phytoplankton biomass integrated in the upper water column was relatively low (∼ 63 mg chl-$a$ m$^{-2}$), but still around 4-folds higher than offshore (∼ 14 mg chl-$a$ m$^{-2}$). This marked difference set the stage for the occurrence over the shelf of a diverse zooplankton community (e.g., Table 3), a dominant herbivorous food chain with a more positive biovolume size-spectrum slope (i.e. dominance of large grazers) and a relatively high secondary production (e.g. nauplii recruitment) when compared with the offshore ecosystem where multivory and recycling appeared to predominate (cf. Darnis et al., 2008). Such a shelf-basin gradient seems to be a well-defined feature of the Western Arctic Ocean as a sharp latitudinal

**Particles and zooplankton in Beaufort Sea**

A. Forest et al.

Title Page

Abstract | Introduction

Conclusions | References

Tables | Figures

⏮ | ⏭

◀ | ▶

Back | Close

Full Screen / Esc

Printer-friendly Version

Interactive Discussion

discontinuity in the abundance of marine snow and zooplankton was also previously observed between the Chukchi/Beaufort shelves and the Canada basin (Ashjian et al., 2005). However, the latter authors invoked lateral advection by the strong along-shelf current to explain the horizontal gradient, whereas our investigation suggests primarily a biological influence. Similarly, Kosobokova and Hirche (2009) surmised that regional variability in local circulation patterns was the main factor determining zooplankton biomass across Eurasian Arctic shelves, but could not exclude that food availability was also important. Therefore, a better examination of particle flux dynamics and carbon cycling in relation with the physical environment and biogeochemical conditions would be needed to determine the actual origin and fate of particulate organic matter and plankton production in the Southeast Beaufort Sea in late summer 2009.

Nevertheless, our results agree well with the study of Tremblay et al. (2011) who observed high mesozooplankton recruitment on the Mackenzie Shelf in 2007–2008 and a steep gradient of productivity ($\sim$ 3–4 times difference) between the shallow shelf and the adjacent offshore area. Such a perspective indeed contrasts with Carmack and Wassmann (2006) who described the Mackenzie Shelf as an ecosystem lacking direct grazing pathways and where zooplankton populations are poorly developed. Rapid pulses and abrupt declines in ecosystem productivity induced by transient shifts in atmospheric forcing are the norm more than the exception in Arctic marine ecosystems. It is thus imperative to monitor sensitive regions such as the Beaufort Sea where a complex setup of environmental factors drives strong physical and ecological gradients. As such, the routine deployment of autonomous imaging instruments, like the Underwater Vision Profiler, can be beneficial for better understanding large-scale patterns and long-term trends in physical-biological coupling and ecosystem function through both observations and models. Our investigation of the size distribution and mean spatial trends of large particles and zooplankton across the Mackenzie Shelf in July–August 2009 illustrated that the combination of automated imaging techniques and traditional sampling methods is a powerful approach to explore the structural diversity and functioning of Arctic ecosystems through the coastal-marine realm.

# Appendix A

## List of stations and metadata

See Table A1.

# References

Alldredge, A. L.: Discarded appendicularian houses as sources of food, surface habitats, and particulate organic matter in planktonic environments, Limnol. Oceanogr., 21, 14–23, 1976.

Appeltans, W., Bouchet, P., Boxshall, G. A., Fauchald, K., Gordon, D. P., Hoeksema, B. W., Poore, G. C. B., van Soest, R. W. M., Stöhr, S., Walter, T. C., and Costello, M. J.: World Register of marine species, available at: http://www.marinespecies.org, 2011.

Ashjian, C. J., Gallager, S. M., and Plourde, S.: Transport of plankton and particles between the Chukchi and Beaufort Seas during summer 2002, described using a Video Plankton Recorder, Deep-Sea Res. Pt. II, 52, 3259–3280, doi:10.1016/j.dsr2.2005.10.012, 2005.

Barber, D. G. and Hanesiak, J. M.: Meteorological forcing of sea ice concentrations in the Southern Beaufort Sea over the period 1979 to 2000, J. Geophys. Res.-Oceans, 109, C06014, doi:10.1029/2003jc002027, 2004.

Boss, E., Twardowski, M. S., and Herring, S.: Shape of the particulate beam attenuation spectrum and its inversion to obtain the shape of the particulate size distribution, Appl. Opt., 40, 4885–4893, doi:10.1364/AO.40.004885, 2001.

Brugel, S., Nozais, C., Poulin, M., Tremblay, J. E., Miller, L. A., Simpson, K. G., Gratton, Y., and Demers, S.: Phytoplankton biomass and production in the Southeastern Beaufort Sea in autumn 2002 and 2003, Mar. Ecol. Prog. Ser., 377, 63–77, 10.3354/meps07808, 2009.

Burd, A. B. and Jackson, G. A.: Particle aggregation, Ann. Rev. Mar. Sci., 1, 65–90, doi:10.1146/annurev.marine.010908.163904, 2009.

Calbet, A.: The trophic roles of microzooplankton in marine systems, ICES J. Mar. Sci., 65, 325–331, doi:10.1093/icesjms/fsn013, 2008.

Campbell, R. G., Sherr, E. B., Ashjian, C. J., Plourde, S., Sherr, B. F., Hill, V., and Stockwell, D. A.: Mesozooplankton prey preference and grazing impact in the Western Arctic Ocean, Deep-Sea Res. Pt. II, 56, 1274–1289, doi:10.1016/j.dsr2.2008.10.027, 2009.

Capriulo, G. M.: Feeding-related ecology of marine protozoa, in: Ecology of Marine Protozoa, edited by: Capriulo, G. M., Oxford University Press, Oxford, 186–259, 1990.

Carmack, E. C. and MacDonald, R. W.: Oceanography of the Canadian Shelf of the Beaufort Sea: a setting for marine life, Arctic, 55(1), 29–45, 2002.

Carmack, E. and Wassmann, P.: Food webs and physical-biological coupling on pan-Arctic shelves: unifying concepts and comprehensive perspectives, Prog. Oceanogr., 71, 446–477, doi:10.1016/j.pocean.2006.10.004, 2006.

**Particles and zooplankton in Beaufort Sea**

A. Forest et al.

Title Page

| Abstract | Introduction |
| Conclusions | References |
| Tables | Figures |

◀◀   ▶▶

◀   ▶

Back   Close

Full Screen / Esc

Printer-friendly Version

Interactive Discussion

Carmack, E. C., Macdonald, R. W., and Jasper, S.: Phytoplankton productivity on the Canadian Shelf of the Beaufort Sea, Mar. Ecol. Prog. Ser., 277, 37–50, 2004.

CIS: Seasonal Summary for the Canadian Arctic – Summer 2009, Canadian Ice Service web site, available at: http://www.ec.gc.ca/Publications, last access: 5 August 2011, 2009.

Crease, J.: The acquisition, calibration and analysis of CTD data. Unesco Technical Papers in Marine Science No. 54, Report of SCOR Working Group 51, Division of Marine Sciences, UNESCO, Paris, 105 pp., 1988.

Darnis, G., Barber, D. G., and Fortier, L.: Sea ice and the onshore-offshore gradient in pre-winter zooplankton assemblages in South-Eastern Beaufort Sea, J. Marine Syst., 74, 994–1011, doi:10.1016/j.jmarsys.2007.09.003, 2008.

Deibel, D.: Feeding and metabolism of Appendicularia, in: The biology of pelagic tunicates, edited by: Bone, Q., Oxford University Press, New York, 139–159, 1998.

Deibel, D. and Daly, K.: Zooplankton processes in arctic and antarctic polynyas, in: Polynyas: Windows to the World, edited by: Smith, W. O. and Barber, D. G., Elsevier, Amsterdam, 271–311, 2007.

Falk-Petersen, S., Mayzaud, P., Kattner, G., Sargent, J. R., and Fenchel, T.: Lipids and life strategy of Arctic Calanus, Mar. Biol. Res., 5, 18–39, doi:10.1080/17451000802512267, 2009.

Folt, C. L. and Burns, C. W.: Biological drivers of zooplankton patchiness, Trends Ecol. Evol., 14, 300–305, doi:10.1016/s0169-5347(99)01616-x, 1999.

Forest, A., Sampei, M., Makabe, R., Sasaki, H., Barber, D., Gratton, Y., Wassmann, P., and Fortier, L.: The annual cycle of particulate organic carbon export in Franklin Bay (Canadian Arctic): environmental control and food web implications, J. Geophys. Res.-Oceans, 113, C03S05, doi:10.1029/2007JC004262, 2008.

Forest, A., Tremblay, J.-É., Gratton, Y., Martin, J., Gagnon, J., Darnis, G., Sampei, M., Fortier, L., Ardyna, M., Gosselin, M., Hattori, H., Nguyen, D., Maranger, R., Vaque, D., Marrase, C., Pedros-Alio, C., Sallon, A., Michel, C., Kellogg, C., Deming, J., Shadwick, E., Thomas, H., Link, H., Archambault, P., and Piepenburg, D.: Biogenic carbon flows through the planktonic food web of the Amundsen Gulf (Arctic Ocean): a synthesis of field measurements and inverse modeling analyses, Prog. Oceanogr., 91(4), 410–436, doi:10.1016/j.pocean.2011.05.002, 2011.

Frangoulis, C., Psarra, S., Zervakis, V., Meador, T., Mara, P., Gogou, A., Zervoudaki, S., Giannakourou, A., Pitta, P., Lagaria, A., Krasakopoulou, E., and Siokou-Frangou, I.: Connecting export fluxes to plankton food-web efficiency in the Black Sea waters inflowing into the

**Particles and zooplankton in Beaufort Sea**

A. Forest et al.

| Title Page | |
|:---:|:---:|
| Abstract | Introduction |
| Conclusions | References |
| Tables | Figures |
| ◄◄ | ►► |
| ◄ | ► |
| Back | Close |
| Full Screen / Esc | |

Printer-friendly Version

Interactive Discussion

Mediterranean Sea, J. Plankton Res., 32, 1203–1216, doi:10.1093/plankt/fbq010, 2010.

Frost, B. W.: *Calanus marshallae*, a new species of calanoid copepod closely allied to the sibling species *C. finmarchicus* and *C. glacialis*, Mar. Biol., 26, 77–99, 1974.

Gordeev, V. V.: Fluvial sediment flux to the Arctic Ocean, Geomorphology, 80, 94–104, doi:10.1016/j.geomorph.2005.09.008, 2006.

Gorsky, G., Ohman, M. D., Picheral, M., Gasparini, S., Stemmann, L., Romagnan, J.-B., Cawood, A., Pesant, S., Garcia-Comas, C., and Prejger, F.: Digital zooplankton image analysis using the ZooScan integrated system, J. Plankton Res., 32, 285–303, doi:10.1093/plankt/fbp124, 2010.

Guidi, L., Jackson, G. A., Stemmann, L., Miquel, J. C., Picheral, M., and Gorsky, G.: Relationship between particle size distribution and flux in the mesopelagic zone, Deep-Sea Res. Pt. I, 55, 1364–1374, doi:10.1016/j.dsr.2008.05.014, 2008.

Guidi, L., Stemmann, L., Jackson, G. A., Ibanez, F., Claustre, H., Legendre, L., Picheral, M., and Gorskya, G.: Effects of phytoplankton community on production, size and export of large aggregates: a world-ocean analysis, Limnol. Oceanogr., 54, 1951–1963, 2009.

Ingram, R. G., Williams, W. J., van Hardenberg, B., Dawe, J. T., and Carmack, E.: Seasonal circulation over the Canadian Beaufort Shelf, in: On Thin Ice: A Synthesis of the Canadian Arctic Shelf Exchange Study (CASES), edited by: Fortier, L., Barber, D. G., and Michaud, J., Aboriginal Issues Press, Winnipeg, 13–38, 2008.

Iversen, M. H., Nowald, N., Ploug, H., Jackson, G. A., and Fischer, G.: High resolution profiles of vertical particulate organic matter export off Cape Blanc, Mauritania: degradation processes and ballasting effects, Deep-Sea Res. Pt. I, 57, 771–784, doi:10.1016/j.dsr.2010.03.007, 2010.

Jackson, G. A. and Checkley Jr, D. M.: Particle size distributions in the upper 100 m water column and their implications for animal feeding in the plankton, Deep-Sea Res. Pt. I, 58, 283-297, doi:10.1016/j.dsr.2010.12.008, 2011.

Karakas, G., Nowald, N., Schefer-Neth, C., Iversen, M., Barkmann, W., Fischer, G., Marchesiello, P., and Schlitzer, R.: Impact of particle aggregation on vertical fluxes of organic matter, Prog. Oceanogr., 83, 331–341, doi:10.1016/j.pocean.2009.07.047, 2009.

Kellogg, C., Carpenter, S., Renfro, A., Sallon, A., Michel, C., Cochran, J., and Deming, J.: Evidence for microbial attenuation of particle flux in the Amundsen Gulf and Beaufort Sea: elevated hydrolytic enzyme activity on sinking aggregates, Polar Biol., 34(12), 2007–2023, doi:10.1007/s00300-011-1015-0, 2011.

**Particles and zooplankton in Beaufort Sea**

A. Forest et al.

Kosobokova, K. and Hirche, H.-J.: Biomass of zooplankton in the Eastern Arctic Ocean: a base line study, Prog. Oceanogr., 82, 265–280, doi:10.1016/j.pocean.2009.07.006, 2009.

Kosobokova, K. N. and Hopcroft, R. R.: Diversity and vertical distribution of meso-zooplankton in the Arctic's Canada Basin, Deep-Sea Res. Pt. II, 57, 96–110, doi:10.1016/j.dsr2.2009.08.009, 2010.

Kosobokova, K. N., Hirche, H.-J., and Scherzinger, T.: Feeding ecology of *Spinocalanus antarcticus*, a mesopelagic copepod with a looped gut, Mar. Biol., 141, 503–511, doi:10.1007/s00227-002-0848-z, 2002.

Kriest, I. and Evans, G. T.: A vertically resolved model for phytoplankton aggregation, P. Indian A.S.-Earth, 109, 453–469, 2000.

Legendre, L. and Michaud, J.: Flux of biogenic carbon in oceans: size-dependent regulation by pelagic food webs, Mar. Ecol. Prog. Ser., 154, 1–11, doi:10.3354/meps164001, 1998.

Li, W. K. W., McLaughlin, F. A., Lovejoy, C., and Carmack, E. C.: Smallest algae thrive as the Arctic Ocean freshens, Science, 326, 539, doi:10.1126/science.1179798, 2009.

Lansard, B., Mucci, A., Miller, L. A., Macdonald, R. W., and Gratton, Y.: Seasonal variability of water mass distribution in the Southeastern Beaufort Sea determined by total alkalinity and $\delta^{18}$O, J. Geophys. Res.-Oceans, submitted, 2011.

Longhurst, A. R.: Relationship between diversity and the vertical structure of the upper ocean, Deep-Sea Res. Pt. I, 32, 1535–1570, doi:10.1016/0198-0149(85)90102-5, 1985.

Macdonald, R. and Yu, Y.: The Mackenzie Estuary of the Arctic Ocean, in: The Handbook of Environmental Chemistry, edited by: Wangersky, P. J., Springer, Berlin, 91–120, 2006.

Martin, J., Tremblay, J. E., Gagnon, J., Tremblay, G., Lapoussière, A., Jose, C., Poulin, M., Gosselin, M., Gratton, Y., and Michel, C.: Prevalence, structure and properties of sub-surface chlorophyll maxima in Canadian Arctic waters, Mar. Ecol. Prog. Ser., 42, 69–84, doi:10.3354/meps08666, 2010.

Mauchline, J.: The biology of calanoid copepods, in: Advances in Marine Biology, edited by: Blaxter, J. and Southward, A., Academic Press, London, 710 pp., 1998.

McDonnell, A. M. P. and Buesseler, K. O.: Variability in the average sinking velocity of marine particles, Limnol. Oceanogr., 55, 2085–2096, 2010.

Moloney, C. L., Jarre, A., Kimura, S., Mackas, D. L., Maury, O., Murphy, E. J., Peterson, W. T., Runge, J. A., and Tadokoro, K.: Dynamics of marine ecosystems: ecological processes, in: Marine Ecosystems and Global Change, doi:10.1093/acprof:oso/9780199558025.001.0001, edited by: Barange, M., Oxford University Press, Oxford, 179–219, 2010.

**Particles and zooplankton in Beaufort Sea**

A. Forest et al.

Title Page

| Abstract | Introduction |
| Conclusions | References |
| Tables | Figures |

|◄ | ►|

◄ | ►

Back | Close

Full Screen / Esc

Printer-friendly Version

Interactive Discussion

O'Brien, M. C., Macdonald, R. W., Melling, H., and Iseki, K.: Particle fluxes and geochemistry on the Canadian Beaufort Shelf: implications for sediment transport and deposition, Cont. Shelf Res., 26, 41–81, doi:10.1016/j.csr.2005.09.007, 2006.

Olli, K., Wassmann, P., Reigstad, M., Ratkova, T. N., Arashkevich, E., Pasternak, A., Matrai, P. A., Knulst, J., Tranvik, L., Klais, R., and Jacobsen, A.: The fate of production in the Central Arctic Ocean – top-down regulation by zooplankton expatriates?, Prog. Oceanogr., 72, 84–113, doi:10.1016/j.pocean.2006.08.002, 2007.

Picheral, M., Guidi, L., Stemmann, L., Karl, D. M., Iddaoud, G., and Gorsky, G.: The Underwater Vision Profiler 5: an advanced instrument for high spatial resolution studies of particle size spectra and zooplankton, Limnol. Oceanogr.-Meth., 8, 462–473, 2010.

Platt, T. and Denman, K. L.: The structure of pelagic marine ecosystems, Rapp. Proces., 173, 60–65, 1978.

Razouls, C., de Bovée, F., Kouwenberg, J., and Desreumaux, N.: Diversity and Geographic Distribution of Marine Planktonic Copepods, available at: http://copepodes.obs-banyuls.fr/en, last access: 20 June 2011, 2005–2011.

Remsen, A., Hopkins, T. L., and Samson, S.: What you see is not what you catch: a comparison of concurrently collected net, Optical Plankton Counter, and Shadowed Image Particle Profiling Evaluation Recorder data from the Northeast Gulf of Mexico, Deep-Sea Res. Pt. I, 51, 129–151, doi:10.1016/j.dsr.2003.09.008, 2004.

Richardson, T. L. and Jackson, G. A.: Small phytoplankton and carbon export from the surface ocean, Science, 315, 838–840, doi:10.1126/science.1133471, 2007.

Sakshaug, E.: Primary and secondary production in the arctic seas, in: The Organic Carbon Cycle in the Arctic Ocean, edited by: Stein, R., and MacDonald, R. W., Springer-Verlag, New-York, 57–81, 2004.

Sampei, M., Forest, A., Sasaki, H., Hattori, H., Makabe, R., Fukuchi, M., and Fortier, L.: Attenuation of the vertical flux of copepod fecal pellets under Arctic sea ice: evidence for an active detrital food web in winter, Polar Biol., 32, 225–232, doi:10.1007/s00300-008-0523-z, 2009.

Seuthe, L., Darnis, G., Riser, C. W., Wassmann, P., and Fortier, L.: Winter–spring feeding and metabolism of Arctic copepods: insights from faecal pellet production and respiration measurements in the Southeastern Beaufort Sea, Polar Biol., 30, 427–436, doi:10.1007/s00300-006-0199-1, 2007.

Stemmann, L. and Boss, E.: Particle and plankton size and packaging: from determining optical properties to driving the biological pump, Ann. Rev. Mar. Sci., 4, 4:18.1-18.27,

**Particles and zooplankton in Beaufort Sea**

A. Forest et al.

doi:10.1146/annurev-marine-120710-100853, 2012.

Stemmann, L., Jackson, G. A., and Ianson, D.: A vertical model of particle size distributions and fluxes in the midwater column that includes biological and physical processes – Part I: model formulation, Deep-Sea Res. Pt. I, 51, 865–884, doi:10.1016/j.dsr.2004.03.001, 2004.

Stemmann, L., Youngbluth, M., Robert, K., Hosia, A., Picheral, M., Paterson, H., Ibanez, F., Guidi, L., Lombard, F., and Gorsky, G.: Global zoogeography of fragile macrozooplankton in the upper 100–1000 m inferred from the underwater video profiler, ICES J. Mar. Sci., 65, 433–442, doi:10.1093/icesjms/fsn010, 2008.

Suzuki, N. and Sato, K.: Studies on suspended particles, marine snow in the sea – I. source of marine snow, B. Fac. Fish. Hokkaido Univ., 4, 132–137, 1953.

Tremblay, J.-É., Bélanger, S., Barber, D. G., Asplin, M., Martin, J., Fortier, L., Darnis, G., Gratton, Y., Link, H., Archambault, P., Williams, W. G., Philippe, B., and Gosselin, M.: Climate forcing multiplies biological productivity in the Arctic Ocean, Geophys. Res. Lett., 38, L18604, doi:10.1029/2011GL048825, 2011.

Tremblay, J.-É., Simpson, K., Martin, J., Miller, L. A., Gratton, Y., and Price, N. M.: Vertical stability and the annual dynamics of nutrients and chlorophyll fluorescence in the coastal, Southeast Beaufort Sea, J. Geophys. Res.-Oceans, 113, C07S90, doi:10.1029/2007JC004547, 2008.

Wassmann, P., Olli, K., Wexels Riser, C., and Svensen, C.: Ecosystem function, biodiversity and vertical flux regulation in the twilight zone, in: Marine Science Frontiers for Europe, edited by: Wefer, G., Lamy, F., and Mantoura, F., Springer Verlag, Berlin, 279–287, 2003.

Wexels Riser, C., Wassmann, P., Reigstad, M., and Seuthe, L.: Vertical flux regulation by zooplankton in the Northern Barents Sea during Arctic spring, Deep-Sea Res. Pt. II, 55, 2320–2329, doi:10.1016/j.dsr2.2008.05.006, 2008.

Zhou, M.: What determines the slope of a plankton biomass spectrum?, J. Plankton Res., 28, 437–448, doi:10.1093/plankt/fbi119, 2006.

Zhou, M., Carlotti, F., and Zhu, Y.: A size-spectrum zooplankton closure model for ecosystem modelling, J. Plankton Res., 32, 1147–1165, doi:10.1093/plankt/fbq054, 2010.

Title Page

Abstract Introduction

Conclusions References

Tables Figures

◄ ►

◄ ►

Back Close

Full Screen / Esc

Printer-friendly Version

Interactive Discussion

**Table 1.** Performance of the automatic recognition for the zooplankton groups analyzed using the ZooScan.

|  | True positive (recall rate) | False positive (contamination rate) |
|---|---|---|
| Appendicularians | 66.7 % | 32.9 % |
| Copepods* | 84.9 % | 19.4 % |
| Detritus | 78.1 % | 20.5 % |
| Carnivorous gelatinous | 63.0 % | 34.3 % |

*Do not include nauplii

Title Page

Abstract    Introduction

Conclusions    References

Tables    Figures

◄    ►

Back    Close

Full Screen / Esc

Printer-friendly Version

Interactive Discussion

**Table 2.** Abundance and biovolume of zooplankton groups (mean ± SE and percent contribution in brackets) as identified and measured using an Underwater Vision Profiler 5 (UVP5) connected to a CTD-rosette profiler and deployed in the shelf ($<100$ m), slope (100–1000 m) and basin ($>1000$ m) regions of Southeast Beaufort Sea in July/August 2009 (Fig. 1). The data presented in this table summarize the entire UVP5 dataset comprising 154 profiles (Appendix A). The vertical distribution of each zooplankton group abundance and biovolume is presented in Fig. 5.

| | Shelf abundance (ind. m$^{-3}$) | Slope abundance (ind. m$^{-3}$) | Basin abundance (ind. m$^{-3}$) |
|---|---|---|---|
| Copepods | 68.4 ± 6.7 (81.8 % ± 8.0 %) | 20.8 ± 2.5 (81.8 % ± 9.9 %) | 7.7 ± 1.0 (84.3 % ± 11.4 %) |
| Appendicularians | 7.4 ± 1.2 (8.8 % ± 1.4 %) | 1.2 ± 0.6 (4.9 % ± 2.2 %) | 0.2 ± 0.1 (1.8 % ± 0.8 %) |
| Chaetognaths | 0.2 ± 0.2 (0.2 % ± 0.2 %) | 0.1 ± 0 (0.5 % ± 1.0 %) | < 0.1 (<0.1 %) |
| Protozoans | 3.1 ± 0.9 (3.7 % ± 1.1 %) | 2.3 ± 0.4 (9.1 % ± 1.5 %) | 0.8 ± 0.2 (9.0 % ± 2.6 %) |
| Ctenophores | 2.0 ± 0.5 (2.4 % ± 0.6 %) | 0.2 ± 0 (0.9 % ± 0.2 %) | 0.1 ± 0 (0.9 % ± 0.4 %) |
| Other gelatinous | 2.6 ± 0.5 (3.1 % ± 0.6 %) | 0.7 ± 0.1 (2.8 % ± 0.4 %) | 0.3 ± 0.1 (3.5 % ± 0.06 %) |
| Total | 83.7 ± 10.0 (100 %) | 25.3 ± 3.6 (100 %) | 9.1 ± 1.4 (100 %) |
| | Shelf biovolume (mm$^3$ m$^{-3}$) | Slope biovolume (mm$^3$ m$^{-3}$) | Basin biovolume (mm$^3$ m$^{-3}$) |
| Copepods | 683.6 ± 185.7 (27.5 % ± 7.5 %) | 119.9 ± 23.7 (21.7 % ± 4.3 %) | 54.9 ± 8.9 (42.2 % ± 6.8 %) |
| Appendicularians | 1412.4 ± 211.9 (56.8 % ± 8.5 %) | 381.5 ± 239.8 (69.1 % ± 43.5 %) | 35.9 ± 17.5 (27.6 % ± 13.5 %) |
| Chaetognaths | 140.3 ± 39.6 (5.6 % ± 1.6 %) | 34.6 ± 10 (6.3 % ± 1.8 %) | 28.7 ± 9.5 (22.1 % ± 7.3 %) |
| Protozoans | 3.0 ± 1.3 (0.1 % ± 0.1 %) | 2.0 ± 0.3 (0.4 % ± 0.1 %) | 0.8 ± 0.2 (0.6 % ± 0.2 %) |
| Ctenophores | 7.3 ± 6.9 (0.3 % ± 0.3 %) | 9.4 ± 3.3 (1.7 % ± 0.6 %) | 1.0 ± 0.7 (0.8 % ± 0.5 %) |
| Other gelatinous | 242.2 ± 121.6 (9.7 % ± 4.9 %) | 4.5 ± 2.2 (0.8 % ± 0.4 %) | 8.9 ± 8.2 (6.8 % ± 6.3 %) |
| Total | 2488.8 ± 567.0 (100 %) | 551.9 ± 279.3 (100 %) | 130.2 ± 45 (100 %) |

**Table 3.** Abundance of sorted zooplankton groups and biovolume of copepodites (including adults; mean ± SE and percent contribution in brackets) as identified by traditional taxonomic counts in samples from integrated vertical net tows (bottom to surface, 200 µm mesh size) conducted in the shelf (< 100 m), slope (100–1000 m) and basin (> 1000 m) regions of Southeast Beaufort Sea in July/August 2009 (Fig. 1). The data presented in this table summarize the whole zooplankton net dataset comprising 29 vertical tows (Appendix A). The biovolume of copepodites was based on the morphometry of copepods for which species-specific body measurements were available (see Sect. 2.3). No morphometric estimates were attempted on other groups. N/A: not available.

| | Shelf abundance (ind. m$^{-3}$) | Slope abundance (ind. m$^{-3}$) | Basin abundance (ind. m$^{-3}$) |
|---|---|---|---|
| Copepods (copepodites*) | 250.9 ± 44.7 (58.6 % ± 10.4 %) | 80.2 ± 10.2 (87 % ± 11 %) | 28.2 ± 6.7 (87.0 % ± 20.7 %) |
| Copepods (nauplii) | 81.4 ± 22.2 (19.0 % ± 5.2 %) | 6.8 ± 1.1 (7.3 % ± 1.3 %) | 1.8 ± 0.6 (5.5 % ± 1.9 %) |
| Appendicularians | 46.9 ± 35.6 (11.0 % ± 8.3 %) | 1.0 ± 0.2 (1.0 % ± 0.2 %) | 0.4 ± 0.1 (1.2 % ± 0.2 %) |
| Echinoderms | 16.4 ± 6.3 (3.8 % ± 1.5 %) | 0.3 ± 0.1 (0.3 % ± 0.1 %) | < 0.1 (<0.1 %) |
| Pteropods | 15.1 ± 5.0 (3.6 % ± 1.2 %) | 0.9 ± 0.1 (1.0 % ± 0.2 %) | 0.6 ± 0.3 (1.9 % ± 0.9 %) |
| Barnacles | 7.5 ± 3.3 (1.7 % ± 0.8 %) | 0.2 ± 0.1 (0.2 % ± 0.1 %) | < 0.1 (<0.1 %) |
| Protozoans | 4.7 ± 2.7 (1.1 % ± 0.6 %) | 0.9 ± 0.4 (1.0 % ± 0.4 %) | 0.5 ± 0.3 (1.5 % ± 0.9 %) |
| Polychaetes | 2.1 ± 0.9 (0.5 % ± 0.2 %) | 0.3 ± 0.1 (0.3 % ± 0.1 %) | 0.1 ± 0.1 (0.3 % ± 0.2 %) |
| Cnidarians | 1.7 ± 0.4 (0.4 % ± 0.1 %) | 0.5 ± 0.1 (0.5 % ± 0.1 %) | 0.1 ± 0.1 (0.4 % ± 0.2 %) |
| Chaetognaths | 1.2 ± 0.7 (0.3 % ± 0.2 %) | 0.3 ± 0.1 (0.3 % ± 0.1 %) | 0.1 ± 0.1 (0.4 % ± 0.1 %) |
| Ostracods | 0.2 ± 0.1 (<0.1 %) | 0.9 ± 0.2 (1.0 % ± 0.2 %) | 0.5 ± 0.2 (1.4 % ± 0.6 %) |
| Other crustaceans | 0.2 ± 0.1 (< 0.1 %) | 0.2 ± 0.1 (0.2 % ± 0.1 %) | 0.1 ± 0.1 (0.2 % ± 0.1 %) |
| Total | 428.3 ± 122.0 (100 %) | 92.4 ± 12.7 (100 %) | 32.4 ± 8.4 (100 %) |
| | Shelf biovolume (mm$^3$ m$^{-3}$) | Slope biovolume (mm$^3$ m$^{-3}$) | Basin biovolume (mm$^3$ m$^{-3}$) |
| Copepods (copepodites*) | 404.3 ± 69.1 (N/A) | 92.5 ± 12.1 (N/A) | 23.6 ± 2.2 (N/A) |

* Stages CI–CVI (include adults)

**Table 4.** Abundance and biovolume of copepods (copepodites, including adults) and appendicularians (mean ± SE and percent contribution in brackets) as estimated with ZooScan analyses on the samples from integrated vertical net tows (bottom to surface, 200 µm mesh size) conducted in the shelf (< 100 m), slope (100–1000 m) and basin (> 1000 m) regions of Southeast Beaufort Sea in July/August 2009 (Fig. 1). The data presented in this table summarize the whole ZooScan dataset comprising 28 samples (Appendix A).

| | Shelf abundance (ind. m$^{-3}$) | Slope abundance (ind. m$^{-3}$) | Basin abundance (ind. m$^{-3}$) |
|---|---|---|---|
| Copepods (copepodites*) | 262.1 ± 65.6 (86.4 % ± 21.6 %) | 75.3 ± 8.1 (91.6 % ± 9.9 %) | 24.9 ± 5 (93.3 % ± 18.9 %) |
| Appendicularians | 21.1 ± 6.9 (6.9 %m ± 2.3 %) | 2.1 ± 0.3 (2.6 % ± 0.3 %) | 0.6 ± 0.1 (2.2 % ± 0.5 %) |
| Carnivorous gelatinous | 20.2 ± 6.2 (6.7 % ± 2.0 %) | 4.7 ± 0.7 (5.8 % ± 0.9 %) | 1.2 ± 0.1 (4.5 % ± 0.4 %) |
| Total | 303.4 ± 78.7 (100 %) | 82.2 ± 9.1 (100 %) | 26.7 ± 5.3 (100 %) |
| | Shelf biovolume (mm$^3$ m$^{-3}$) | Slope biovolume (mm$^3$ m$^{-3}$) | Basin biovolume (mm$^3$ m$^{-3}$) |
| Copepods (copepodites*) | 456.4 ± 105.2 (64 % ± 14.8 %) | 125.6 ± 19.9 (60.5 % ± 9.6 %) | 65.4 ± 13.3 (75.7 % ± 15.5 %) |
| Appendicularians | 135.9 ± 47.2 (19.1 % ± 6.6 %) | 8.3 ± 1.2 (4.0 % ± 0.6 %) | 2.3 ± 5.8 (2.7 % ± 6.7 %) |
| Carnivorous gelatinous | 120.4 ± 55.2 (16.9 % ± 7.7 %) | 73.6 ± 30.8 (35.5 % ± 14.9 %) | 18.6 ± 6.3 (21.6 % ± 7.4 %) |
| Total | 712.6 ± 207.5 (100 %) | 207.5 ± 51.9 (100 %) | 86.3 ± 25.4 (100 %) |

* Stages CI–CVI (include adults)

**Particles and zooplankton in Beaufort Sea**

A. Forest et al.

Title Page

Abstract | Introduction

Conclusions | References

Tables | Figures

◀ | ▶

◀ | ▶

Back | Close

Full Screen / Esc

Printer-friendly Version

Interactive Discussion

**Table A1.** List and metadata of oceanographic stations where sampling using an Underwater Vision Profiler 5 and traditional zooplankton nets was conducted in the Southeast Beaufort Sea in July/August 2009 as part of the successive ArcticNet and Malina campaigns. Data from multiple UVP5 profiles conducted at each of the overlapping stations were averaged in order to perform comparisons with the vertical net tow dataset.

| Cruise | Station | Date (UTC) | Time (UTC) | Latitude (°N) | Longitude (°W) | Bottom depth(m) | UVP5 profile | Zooplankton net Taxonomy | ZooScan |
|---|---|---|---|---|---|---|---|---|---|
| ArcticNet | 1 | 18-Jul-09 | 11:45:36 | 70.48 | 135.11 | 62 | X | X | X |
| ArcticNet | 1 | 18-Jul-09 | 12:00:00 | 70.48 | 135.12 | 62 | X | | |
| ArcticNet | 2 | 19-Jul-09 | 00:28:48 | 70.66 | 135.64 | 148 | X | X | X |
| ArcticNet | 11 | 19-Jul-09 | 06:14:24 | 70.74 | 135.56 | 363 | X | X | X |
| ArcticNet | 11 | 19-Jul-09 | 08:24:00 | 70.74 | 135.54 | 363 | X | | |
| ArcticNet | 3 | 19-Jul-09 | 12:57:36 | 70.71 | 135.8 | 400 | X | X | X |
| ArcticNet | 14 | 20-Jul-09 | 00:28:48 | 70.58 | 135.48 | 94 | X | X | X |
| ArcticNet | 15 | 20-Jul-09 | 06:28:48 | 70.65 | 135.93 | 294 | X | X | X |
| ArcticNet | 17 | 20-Jul-09 | 12:57:36 | 70.61 | 136.47 | 730 | X | X | X |
| ArcticNet | 4 | 21-Jul-09 | 02:38:24 | 70.76 | 136.02 | 688 | X | X | X |
| ArcticNet | 10 | 21-Jul-09 | 12:43:12 | 70.79 | 135.53 | 432 | X | X | X |
| ArcticNet | I-09 | 21-Jul-09 | 21:50:24 | 70.82 | 134.55 | 73 | X | | |
| ArcticNet | 23 | 22-Jul-09 | 00:57:36 | 70.9 | 134.27 | 82 | X | X | X |
| ArcticNet | 22 | 22-Jul-09 | 07:40:48 | 70.82 | 134.51 | 72 | X | X | X |
| ArcticNet | 21 | 22-Jul-09 | 16:33:36 | 71.02 | 134.63 | 337 | X | X | X |
| ArcticNet | 18 | 23-Jul-09 | 01:12:00 | 70.88 | 135.36 | 495 | X | X | X |
| ArcticNet | 8 | 23-Jul-09 | 07:40:48 | 70.92 | 135.86 | 782 | X | X | X |
| ArcticNet | 20 | 23-Jul-09 | 15:50:24 | 71.02 | 135.35 | 645 | X | X | X |
| ArcticNet | 16 | 24-Jul-09 | 14:09:36 | 70.8 | 136.66 | 1084 | X | X | X |
| ArcticNet | 6 | 25-Jul-09 | 06:57:36 | 70.94 | 136.43 | 1024 | X | X | X |
| ArcticNet | 7 | 25-Jul-09 | 14:24:00 | 70.99 | 136.13 | 1018 | X | X | X |
| ArcticNet | M-09 | 26-Jul-09 | 02:52:48 | 70.74 | 135.92 | 583 | X | X | X |
| ArcticNet | 13 | 27-Jul-09 | 03:50:24 | 70.5 | 135.67 | 66 | X | X | X |
| ArcticNet | 12 | 27-Jul-09 | 14:09:36 | 70.64 | 135.1 | 61 | X | X | X |
| Malina | 390 | 31-Jul-09 | 21:07:12 | 70.18 | 133.56 | 58 | X | | |
| Malina | 390 | 31-Jul-09 | 23:02:24 | 70.18 | 133.57 | 40 | X | | |
| Malina | 390 | 1-Aug-09 | 00:28:48 | 70.18 | 133.58 | 43 | X | | |
| Malina | 689 | 1-Aug-09 | 12:28:48 | 69.49 | 137.94 | 52 | X | | |
| Malina | 690 | 1-Aug-09 | 15:07:12 | 69.49 | 137.93 | 51 | X | | |
| Malina | 690 | 1-Aug-09 | 16:48:00 | 69.47 | 137.95 | 53 | X | | |
| Malina | 690 | 1-Aug-09 | 20:24:00 | 69.49 | 137.94 | 55 | X | | |
| Malina | 680 | 2-Aug-09 | 16:48:00 | 69.61 | 138.21 | 120 | X | | |
| Malina | 680 | 2-Aug-09 | 19:12:00 | 69.61 | 138.22 | 122 | X | | |
| Malina | 680 | 2-Aug-09 | 20:52:48 | 69.61 | 138.22 | 124 | X | | |
| Malina | 680 | 2-Aug-09 | 22:48:00 | 69.61 | 138.24 | 124 | X | | |
| Malina | 260 | 4-Aug-09 | 22:04:48 | 71.27 | 130.61 | 54 | X | X | X |
| Malina | 260 | 5-Aug-09 | 00:00:00 | 71.27 | 130.6 | 59 | X | | |
| Malina | 250 | 5-Aug-09 | 04:19:12 | 71.47 | 130.7 | 219 | X | | |
| Malina | 240 | 5-Aug-09 | 06:14:24 | 71.67 | 130.74 | 462 | X | X | X |
| Malina | 230 | 5-Aug-09 | 08:09:36 | 71.87 | 130.84 | 702 | X | | |
| Malina | 220 | 5-Aug-09 | 10:19:12 | 72.06 | 130.89 | 890 | X | | |
| Malina | 220 | 5-Aug-09 | 14:09:36 | 72.05 | 130.83 | 834 | X | | |
| Malina | 220 | 5-Aug-09 | 15:50:24 | 72.05 | 130.88 | 880 | X | | |
| Malina | 220 | 5-Aug-09 | 17:31:12 | 72.05 | 130.94 | 911 | X | | |
| Malina | 240 | 5-Aug-09 | 22:19:12 | 71.67 | 130.73 | 465 | X | | |
| Malina | 240 | 6-Aug-09 | 00:28:48 | 71.67 | 130.74 | 455 | X | | |
| Malina | 110 | 6-Aug-09 | 11:02:24 | 71.7 | 126.48 | 400 | X | | |
| Malina | 110 | 6-Aug-09 | 15:21:36 | 71.7 | 126.48 | 397 | X | | |
| Malina | 110 | 6-Aug-09 | 18:00:00 | 71.7 | 126.48 | 395 | X | | |
| Malina | 120 | 6-Aug-09 | 23:02:24 | 71.57 | 126.91 | 419 | X | | |
| Malina | 130 | 7-Aug-09 | 00:57:36 | 71.43 | 127.37 | 311 | X | X | X |
| Malina | 130 | 7-Aug-09 | 03:36:00 | 71.42 | 127.36 | 313 | X | | |
| Malina | 140 | 7-Aug-09 | 09:07:12 | 71.28 | 127.79 | 140 | X | | |
| Malina | 150 | 7-Aug-09 | 11:16:48 | 71.16 | 128.16 | 66 | X | | |
| Malina | 160 | 7-Aug-09 | 12:43:12 | 71.05 | 128.5 | 43 | X | | |
| Malina | 170 | 7-Aug-09 | 14:38:24 | 70.91 | 128.92 | 35 | X | | |
| Malina | 170 | 7-Aug-09 | 16:19:12 | 70.92 | 128.92 | 35 | X | | |
| Malina | 170 | 7-Aug-09 | 17:45:36 | 70.92 | 128.92 | 35 | X | | |
| Malina | 150 | 7-Aug-09 | 23:02:24 | 71.16 | 128.16 | 66 | X | | |
| Malina | 150 | 8-Aug-09 | 01:12:00 | 71.16 | 128.16 | 66 | X | | |
| Malina | 390 | 8-Aug-09 | 11:31:12 | 70.18 | 133.56 | 44 | X | | |
| Malina | 380 | 8-Aug-09 | 13:12:00 | 70.4 | 133.61 | 60 | X | | |
| Malina | 380 | 8-Aug-09 | 14:52:48 | 70.4 | 133.6 | 63 | X | | |
| Malina | 380 | 8-Aug-09 | 16:19:12 | 70.39 | 133.6 | 62 | X | | |
| Malina | 370 | 8-Aug-09 | 19:12:00 | 70.6 | 133.65 | 70 | X | | |
| Malina | 360 | 8-Aug-09 | 22:04:48 | 70.8 | 133.73 | 75 | X | | |
| Malina | 360 | 8-Aug-09 | 23:31:12 | 70.8 | 133.73 | 74 | X | | |
| Malina | 350 | 9-Aug-09 | 04:19:12 | 70.97 | 133.73 | 90 | X | | |
| Malina | 340 | 9-Aug-09 | 06:28:48 | 71.17 | 133.83 | 575 | X | | |
| Malina | 330 | 9-Aug-09 | 08:09:36 | 71.37 | 133.89 | 1080 | X | | |
| Malina | 320 | 9-Aug-09 | 10:19:12 | 71.57 | 133.94 | 1159 | X | | |
| Malina | 310 | 9-Aug-09 | 12:43:12 | 71.74 | 133.95 | 1614 | X | | |
| Malina | 320 | 9-Aug-09 | 15:07:12 | 71.57 | 133.95 | 1160 | X | | |
| Malina | 320 | 9-Aug-09 | 17:02:24 | 71.56 | 133.95 | 1141 | X | | |
| Malina | 320 | 9-Aug-09 | 18:57:36 | 71.56 | 133.95 | 1115 | X | | |
| Malina | 330 | 9-Aug-09 | 21:36:00 | 71.37 | 133.89 | 1080 | X | | |
| Malina | 340 | 9-Aug-09 | 23:45:36 | 71.17 | 133.82 | 590 | X | | |

| Cruise | Station | Date (UTC) | Time (UTC) | Latitude (°N) | Longitude (°W) | Bottom depth(m) | UVP5 profile | Zooplankton net Taxonomy | ZooScan |
|---|---|---|---|---|---|---|---|---|---|
| Malina | 670 | 10-Aug-09 | 19:26:24 | 69.8 | 138.44 | 172 | X | | |
| Malina | 670 | 10-Aug-09 | 21:07:12 | 69.8 | 138.44 | 174 | X | | |
| Malina | 670 | 10-Aug-09 | 22:48:00 | 69.8 | 138.43 | 173 | X | | |
| Malina | 660 | 11-Aug-09 | 00:57:36 | 69.99 | 138.65 | 268 | X | | |
| Malina | 660 | 11-Aug-09 | 03:21:36 | 69.97 | 138.64 | 260 | X | | |
| Malina | 650 | 11-Aug-09 | 05:31:12 | 70.17 | 138.91 | 374 | X | | |
| Malina | 640 | 11-Aug-09 | 07:40:48 | 70.34 | 139.15 | 564 | X | X | X |
| Malina | 630 | 11-Aug-09 | 09:07:12 | 70.53 | 139.38 | 840 | X | | |
| Malina | 610 | 11-Aug-09 | 14:24:00 | 70.8 | 139.6 | 1823 | X | | |
| Malina | 620 | 11-Aug-09 | 22:48:00 | 70.67 | 139.63 | 1538 | X | | |
| Malina | 630 | 12-Aug-09 | 00:57:36 | 70.53 | 139.37 | 840 | X | | |
| Malina | 640 | 12-Aug-09 | 02:52:48 | 70.34 | 139.14 | 573 | X | | |
| Malina | 760 | 12-Aug-09 | 13:55:12 | 70.55 | 140.8 | 579 | X | | |
| Malina | 760 | 12-Aug-09 | 15:21:36 | 70.55 | 140.8 | 560 | X | | |
| Malina | 760 | 12-Aug-09 | 16:48:00 | 70.55 | 140.79 | 566 | X | | |
| Malina | 760 | 12-Aug-09 | 19:12:00 | 70.54 | 140.78 | 644 | X | | |
| Malina | 770 | 12-Aug-09 | 23:02:24 | 70.35 | 140.81 | 223 | X | | |
| Malina | 780 | 13-Aug-09 | 01:55:12 | 70.15 | 140.81 | 49 | X | | |
| Malina | 780 | 13-Aug-09 | 03:36:00 | 70.15 | 140.8 | 50 | X | | |
| Malina | 345 | 14-Aug-09 | 16:19:12 | 71.33 | 132.56 | 479 | X | | |
| Malina | 345 | 14-Aug-09 | 18:14:24 | 71.34 | 132.59 | 502 | X | | |
| Malina | 345 | 14-Aug-09 | 20:24:00 | 71.35 | 132.61 | 517 | X | | |
| Malina | 345 | 14-Aug-09 | 22:19:12 | 71.35 | 132.61 | 530 | X | | |
| Malina | 345 | 15-Aug-09 | 00:28:48 | 71.35 | 132.62 | 519 | X | X | X |
| Malina | 345 | 15-Aug-09 | 02:24:00 | 71.36 | 132.62 | 520 | X | | |
| Malina | 345 | 15-Aug-09 | 04:19:12 | 71.35 | 132.61 | 524 | X | | |
| Malina | 345 | 15-Aug-09 | 06:14:24 | 71.36 | 132.61 | 536 | X | | |
| Malina | 345 | 15-Aug-09 | 08:09:36 | 71.36 | 132.61 | 539 | X | | |
| Malina | 345 | 15-Aug-09 | 10:19:12 | 71.35 | 132.59 | 519 | X | | |
| Malina | 345 | 15-Aug-09 | 12:14:24 | 71.36 | 132.58 | 525 | X | | |
| Malina | 345 | 15-Aug-09 | 14:24:00 | 71.37 | 132.69 | 559 | X | | |
| Malina | 345 | 15-Aug-09 | 16:19:12 | 71.38 | 132.72 | 612 | X | | |
| Malina | 345 | 15-Aug-09 | 18:28:48 | 71.39 | 132.66 | 602 | X | | |
| Malina | 345 | 15-Aug-09 | 20:24:00 | 71.41 | 132.64 | 580 | X | | |
| Malina | 345 | 15-Aug-09 | 22:19:12 | 71.42 | 132.62 | 619 | X | | |
| Malina | 345 | 16-Aug-09 | 00:28:48 | 71.42 | 132.59 | 625 | X | | |
| Malina | 345 | 16-Aug-09 | 02:24:00 | 71.41 | 132.58 | 602 | X | | |
| Malina | 345 | 16-Aug-09 | 04:19:12 | 71.43 | 132.61 | 654 | X | | |
| Malina | 570 | 17-Aug-09 | 10:48:00 | 70.21 | 137.26 | 55 | X | | |
| Malina | 560 | 17-Aug-09 | 12:14:24 | 70.39 | 137.48 | 400 | X | | |
| Malina | 550 | 17-Aug-09 | 14:09:36 | 70.57 | 137.71 | 1077 | X | | |
| Malina | 540 | 17-Aug-09 | 17:16:48 | 70.75 | 137.89 | 1514 | X | X | X |
| Malina | 540 | 17-Aug-09 | 20:09:36 | 70.76 | 137.89 | 1514 | X | | |
| Malina | 540 | 17-Aug-09 | 22:04:48 | 70.76 | 137.87 | 1522 | X | | |
| Malina | 530 | 18-Aug-09 | 04:33:36 | 70.94 | 138.15 | 1602 | X | | |
| Malina | 430 | 18-Aug-09 | 15:07:12 | 71.22 | 136.71 | 1361 | X | | |
| Malina | 430 | 18-Aug-09 | 17:31:12 | 71.2 | 136.74 | 1334 | X | | |
| Malina | 430 | 19-Aug-09 | 19:26:24 | 71.18 | 136.75 | 1300 | X | | |
| Malina | 440 | 19-Aug-09 | 00:14:24 | 71.04 | 136.46 | 1149 | X | | |
| Malina | 450 | 19-Aug-09 | 02:24:00 | 70.86 | 136.24 | 840 | X | | |
| Malina | 480 | 19-Aug-09 | 07:26:24 | 70.28 | 135.75 | 60 | X | | |
| Malina | 460 | 19-Aug-09 | 13:40:48 | 70.68 | 136.05 | 468 | X | | |
| Malina | 460 | 19-Aug-09 | 15:50:24 | 70.68 | 135.99 | 434 | X | X | X |
| Malina | 460 | 19-Aug-09 | 16:19:12 | 70.68 | 135.97 | 420 | X | | |
| Malina | 460 | 19-Aug-09 | 18:14:24 | 70.68 | 135.89 | 362 | X | | |
| Malina | 135 | 20-Aug-09 | 18:43:12 | 71.31 | 127.48 | 231 | X | | |
| Malina | 135 | 20-Aug-09 | 20:24:00 | 71.31 | 127.49 | 230 | X | | |
| Malina | 135 | 20-Aug-09 | 22:48:00 | 71.31 | 127.49 | 228 | X | | |
| Malina | 135 | 21-Aug-09 | 00:28:48 | 71.31 | 127.5 | 223 | X | | |
| Malina | 135 | 21-Aug-09 | 02:24:00 | 71.31 | 127.49 | 230 | X | | |
| Malina | 135 | 21-Aug-09 | 04:19:12 | 71.31 | 127.49 | 231 | X | | |
| Malina | 135 | 21-Aug-09 | 06:14:24 | 71.31 | 127.5 | 228 | X | | |
| Malina | 135 | 21-Aug-09 | 08:24:00 | 71.31 | 127.49 | 227 | X | | |
| Malina | 135 | 21-Aug-09 | 10:19:12 | 71.31 | 127.49 | 230 | X | | |
| Malina | 135 | 21-Aug-09 | 12:57:36 | 71.31 | 127.49 | 227 | X | | |
| Malina | 135 | 21-Aug-09 | 14:24:00 | 71.31 | 127.5 | 224 | X | | |
| Malina | 135 | 21-Aug-09 | 16:19:12 | 71.31 | 127.5 | 222 | X | | |
| Malina | 135 | 21-Aug-09 | 18:28:48 | 71.31 | 127.49 | 227 | X | | |
| Malina | 135 | 21-Aug-09 | 20:24:00 | 71.31 | 127.5 | 227 | X | | |
| Malina | 135 | 21-Aug-09 | 22:48:00 | 71.31 | 127.5 | 225 | X | | |
| Malina | 235 | 22-Aug-09 | 08:38:24 | 71.76 | 130.83 | 619 | X | X | X |
| Malina | 235 | 22-Aug-09 | 10:48:00 | 71.76 | 130.76 | 567 | X | | |
| Malina | 235 | 22-Aug-09 | 12:14:24 | 71.76 | 130.81 | 599 | X | | |
| Malina | 235 | 22-Aug-09 | 14:09:36 | 71.77 | 130.8 | 598 | X | | |
| Malina | 235 | 22-Aug-09 | 16:19:12 | 71.76 | 130.83 | 617 | X | | |
| Malina | 235 | 22-Aug-09 | 18:28:48 | 71.77 | 130.9 | 666 | X | | |
| Malina | 235 | 22-Aug-09 | 20:24:00 | 71.77 | 130.94 | 681 | X | | |

**Fig. 1.** Bathymetric map of the Southeast Beaufort Sea (Arctic Ocean) with position of the sampling stations conducted in July/August 2009 as part of the successive ArcticNet and Malina campaigns. The ArcticNet sampling sites were located in the exploration license area EL446, whereas transects 100–700 and station 345 correspond to the Malina sampling grid. The shelf, slope and basin regions as defined in the present study correspond to the sampling stations located within the < 100 m, 100–1000 m and > 1000 m isobaths, respectively. The metadata (coordinates, date, sampling type) for each oceanographic station are detailed in the Appendix A.
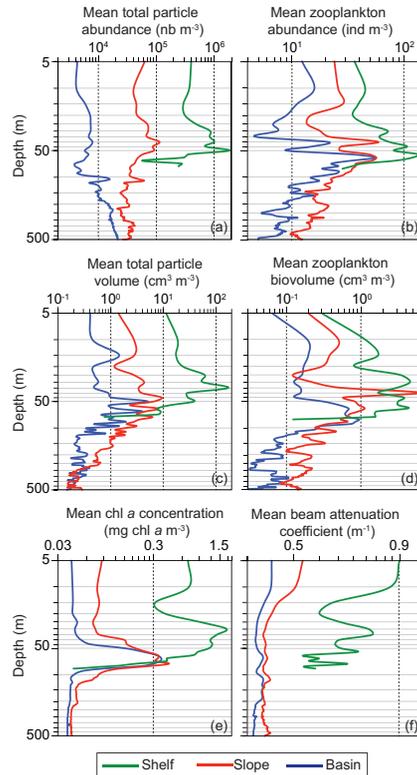
**Fig. 2.** Mean vertical profiles of total particle abundance **(a)**, total zooplankton abundance **(b)**, total particle volume **(c)**, and total zooplankton biovolume **(d)**, as measured with the Underwater Vision Profiler deployed across the shelf ($< 100$ m), slope (100–1000 m) and basin ($> 1000$ m) areas of Southeast Beaufort Sea in July/August 2009 (Fig. 1). The bottom panels present the mean vertical profiles of chlorophyll-*a* concentration **(e)** and beam attenuation coefficient **(f)** as recorded in the same regions and smoothed over 5-m depth.

Title Page

Abstract | Introduction

Conclusions | References

Tables | Figures

|◄ | ►|

◄ | ►

Back | Close

Full Screen / Esc

Printer-friendly Version

Interactive Discussion
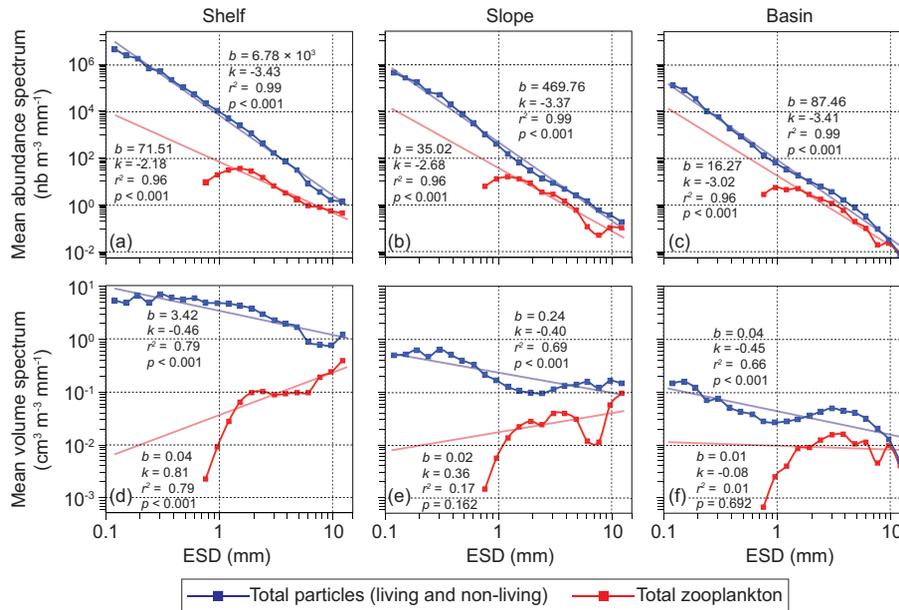
**Fig. 3.** Mean size spectra of abundance **(a–c)** and volume **(d–f)** of total particles and total zooplankton as measured with the Underwater Vision Profiler deployed across the shelf (< 100 m), slope (100–1000 m), and basin (> 1000 m) regions of Southeast Beaufort Sea in July/August 2009 (Fig. 1). The $b$ and $k$ values correspond, respectively, to the constants and scaling exponents (slopes in a log-log form) of the power-law equations ($n = bd^k$) derived from the normalized particle size distributions (see Sect. 2.2 for details). The power-law relationships for total particles were calculated using the full range of 0.1–12 mm (expressed in equivalent spherical diameter, ESD), whereas the equations for zooplankton were calculated using only the organisms > 1 mm ESD because of the loss in the efficiency of detection in the low end (≤ 1 mm ESD) of the zooplankton size spectrum. The percent contributions of living particles to total particles as estimated with the idealized power-law equations are presented in Fig. 4.
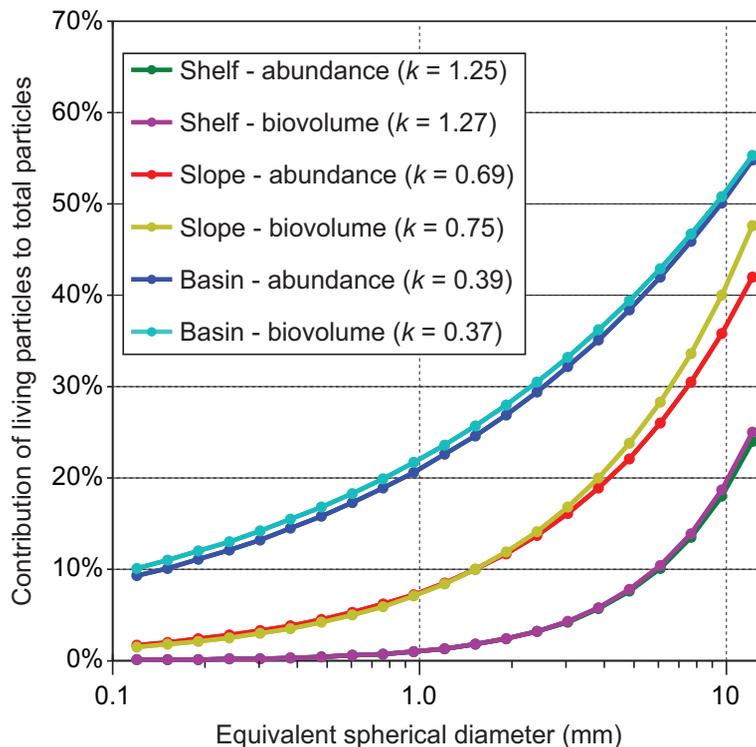
**Fig. 4.** Contribution of living particles (i.e. plankton) to total particle abundance and biovolume across the three target regions as estimated with the power-law equations derived from the normalized particle size distributions acquired with the Underwater Vision Profiler (Fig. 3). This figure aims at showing the idealized percentage of planktonic particulates in the total particle inventory as a function of size expressed in terms of equivalent spherical diameter (ESD). The $k$ value of each curve represents the scaling exponent of the power-law regression (i.e. slope in log-log scale) between the percent contributions of living particles and the various size classes.
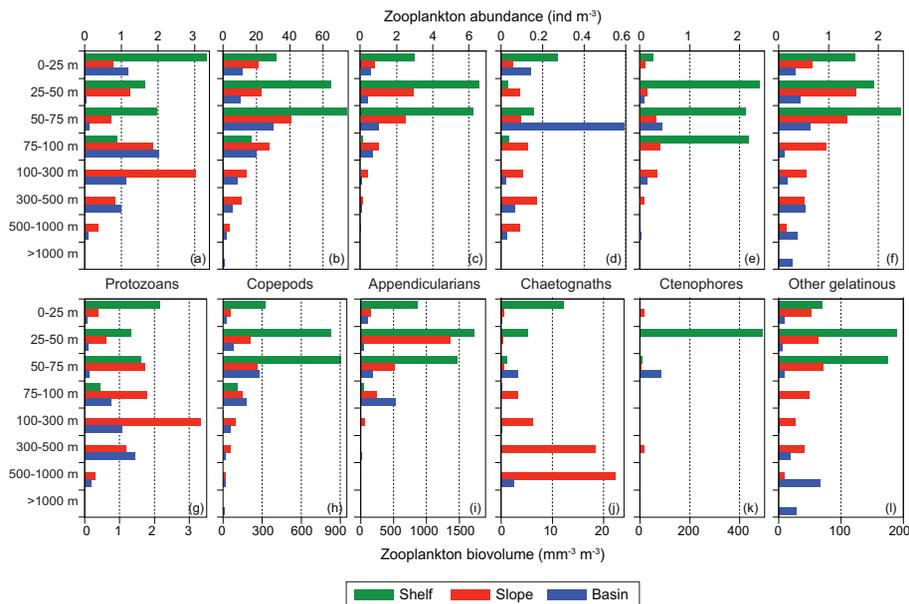
**Fig. 5.** Vertical distribution of zooplankton group abundance **(a–f)** and biovolume **(g–l)** as identified and measured with the Underwater Vision Profiler (UVP) across the shelf (< 100 m), slope (100–1000 m) and basin (> 1000 m) areas of Southeast Beaufort Sea in July/August 2009. The zooplankton abundance and biovolume obtained with the UVP and averaged for the entire water column within each of the defined regions are presented in Table 3.

Title Page

Abstract | Introduction

Conclusions | References

Tables | Figures

◄ | ►►

◄ | ►

Back | Close

Full Screen / Esc

Printer-friendly Version

Interactive Discussion
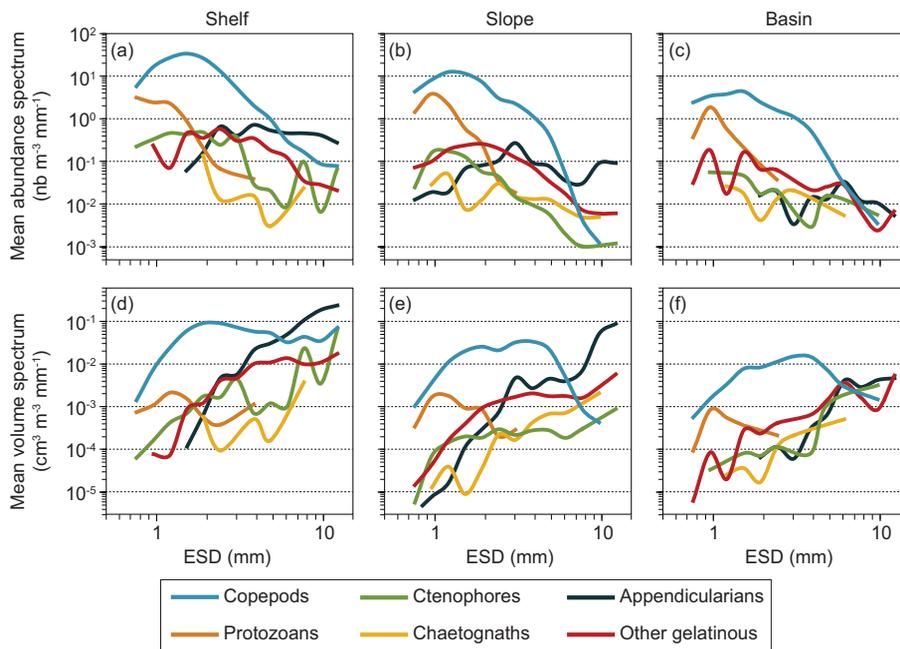
**Fig. 6.** Mean size spectra of abundance **(a–c)** and biovolume **(d–f)** for each zooplankton group as identified and measured with the Underwater Vision Profiler deployed across the shelf-slope-basin interface in the Southeast Beaufort Sea in July/August 2009. ESD: equivalent spherical diameter.
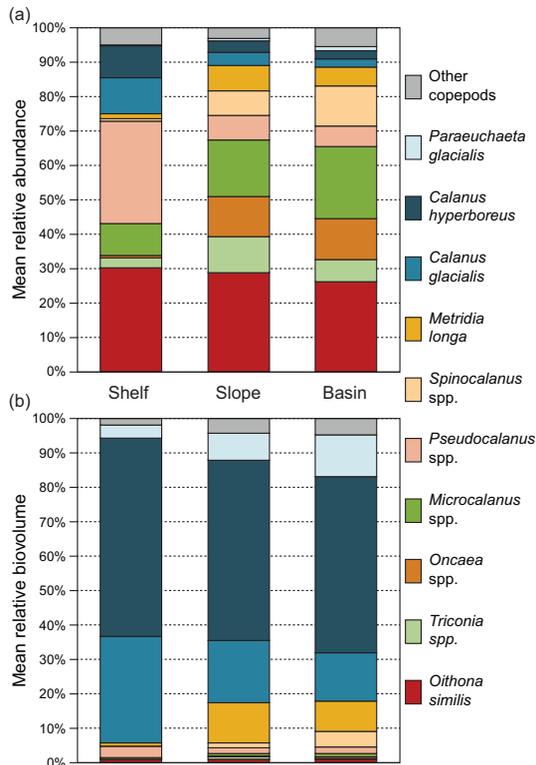
**Fig. 7.** Relative contribution of dominant copepod species in the total abundance **(a)** and biovolume **(b)** of copepod assemblages (copepodites only) as estimated with bottom-to-surface vertical net tows (200 µm mesh size) conducted across the shelf-slope-basin interface in the Southeast Beaufort Sea in July/August 2009. The biovolume of each species was estimated using morphometric estimates based on mean prosome and urosome lengths/widths of each copepodite stage (see Sect. 2.3 for details).

Title Page

Abstract | Introduction

Conclusions | References

Tables | Figures

|◄ | ►|

◄ | ►

Back | Close

Full Screen / Esc

Printer-friendly Version

Interactive Discussion
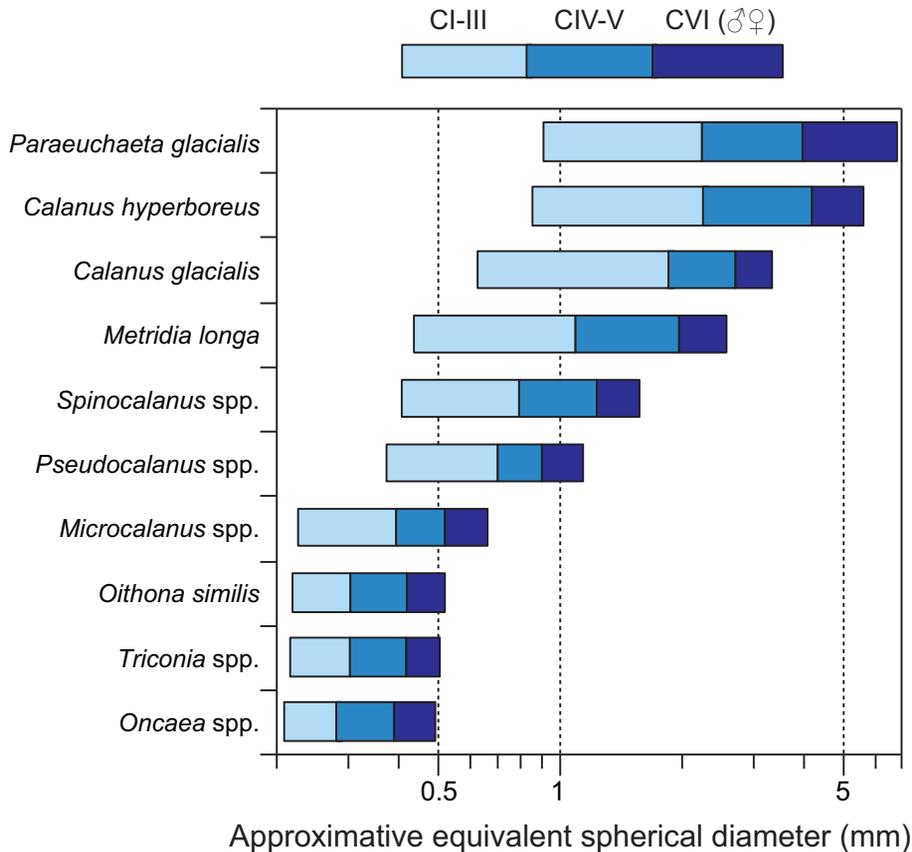
**Fig. 8.** Approximative equivalent spherical diameter (ESD) of each dominant copepod species (Fig. 7) as estimated with morphometric relationships (see Sect. 2.3 for details).

Discussion Paper | Discussion Paper | Discussion Paper | Discussion Paper |

**BGD**

8, 11405–11452, 2011

**Particles and zooplankton in Beaufort Sea**

A. Forest et al.

Title Page

Abstract | Introduction

Conclusions | References

Tables | Figures

|◄ | ►|

◄ | ►

Back | Close

Full Screen / Esc

Printer-friendly Version

Interactive Discussion

**BGD**

8, 11405–11452, 2011

**Particles and zooplankton in Beaufort Sea**

A. Forest et al.

Title Page

| Abstract | Introduction |
| Conclusions | References |
| Tables | Figures |

|◄ | ►|

◄ | ►

Back | Close

Full Screen / Esc

Printer-friendly Version

Interactive Discussion

**Fig. 9.** Average size spectra of abundance **(a–c)** and biovolume **(d–f)** of the total copepod assemblage as estimated using traditional zooplankton nets (further divided into manual estimates and ZooScan measurements) and Underwater Vision Profiler deployments conducted at each of the overlapping stations (Fig. 1, Appendix A) across the shelf (< 100 m), slope (100–1000 m), and basin (> 1000 m) regions of Southeast Beaufort Sea in July/August 2009. The parameters of the power-law equations ($n = bd^k$) derived from size distributions were calculated with the combined datasets (see Sect. 2.3 for details). In each panel, the percent contribution of copepods < 1 mm and > 1 mm to total abundance or biovolume (i.e. sum of all size-classes) is also given according to each methodology. ESD: equivalent spherical diameter.
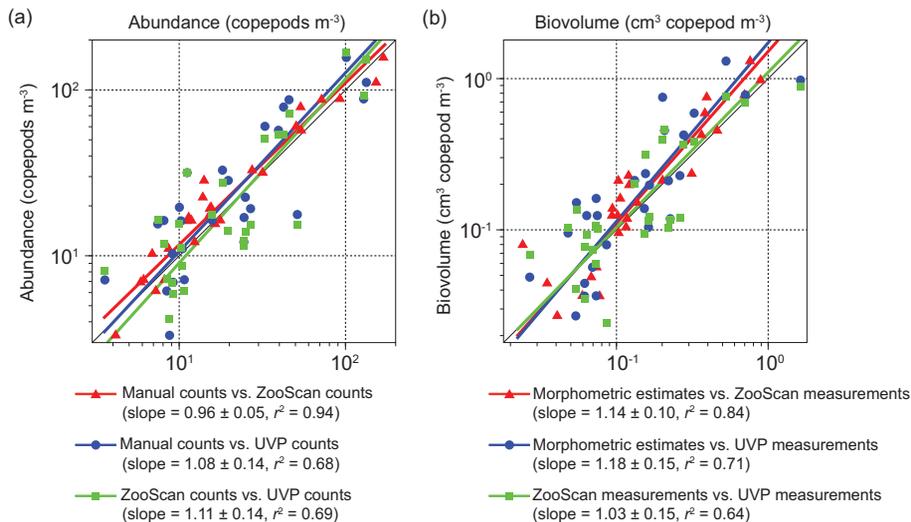
**Fig. 10.** Linear regressions of the log-transformed mean abundance **(a)** and biovolume **(b)** of all copepods within the size range of 1–6 mm (equivalent spherical diameter) as estimated with traditional zooplankton net tows (further divided into manual and ZooScan estimates) and the Underwater Vision Profiler deployed at each of the overlapping stations (Fig. 1, Appendix A).
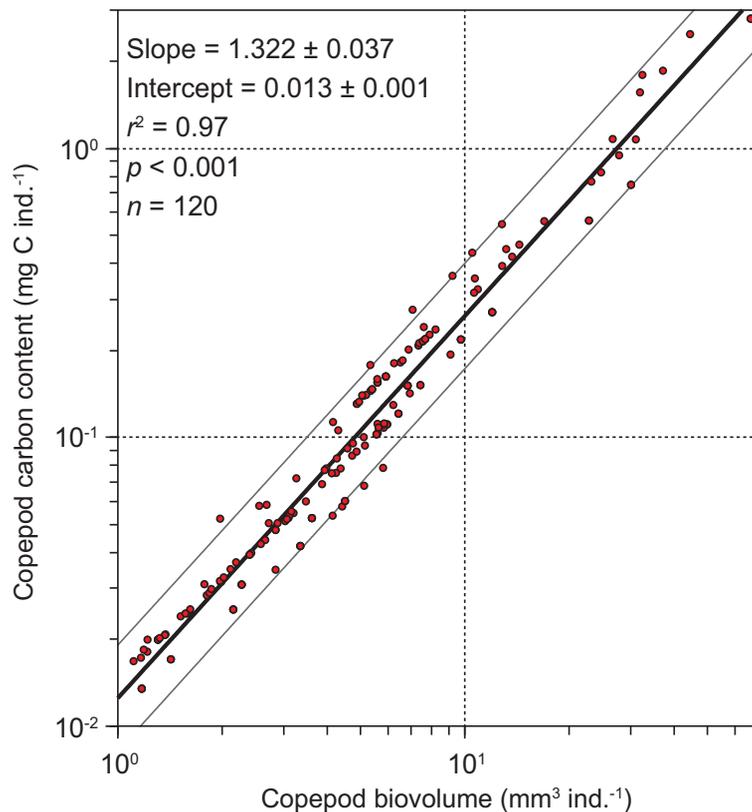
**Fig. 11.** Regression of the empirical carbon content of each copepod stage in the size range 1–6 mm (equivalent spherical diameter) present in the Beaufort Sea against its biovolume as estimated with morphometric relationships (see Sect. 4.2 for related discussion). This regression aims at providing a specific biovolume-to-carbon conversion factor for large Arctic copepods in order to estimate most accurately the copepod biomass with the Underwater Vision Profiler 5 in the Beaufort Sea, and in the Arctic Ocean in general.

Discussion Paper | Discussion Paper | Discussion Paper | Discussion Paper

Title Page

Abstract | Introduction

Conclusions | References

Tables | Figures

◄ | ►

◄ | ►

Back | Close

Full Screen / Esc

Printer-friendly Version

Interactive Discussion